UNIVERSITÀ DI PISA

DIPARTIMENTO DI FARMACIA

Corso di Laurea Specialistica in Chimica e Tecnologia Farmaceutiche

TESI DI LAUREA

DEVELOPMENT OF NOVEL BENZOTHIOPYRANOINDOLE-BASED TDP1 INHIBITORS FOR ANTICANCER THERAPY

Relatori:

Prof.ssa Sabrina Taliani

Dott.ssa Elisabetta Barresi

Candidata:

Elisa Macrelli

Anno Accademico 2015/2016

Index

Preface

1. CANCER.

Cell division (proliferation) is a physiologic process that occurs in almost all tissues and in countless circumstances. Normally, homeostasis, the balance between proliferation and programmed cell death (usually by apoptosis), is strictly maintained by adjusting both processes to ensure the integrity of organs and tissues [1]. Mutations of DNA, which generate cancer cells, destroy these orderly processes by smashing regulator programs. A tumor is characterized by an aberrant structure and uncontrolled cell growth. The alterations that transform normal cells into neoplastic cells are usually structural (mutations) or, more rarely, functional [2].

Genetic mutations that cause cancer are based on three classes of genes:

▪ **Oncogenes**: produced when normal genes, known as proto-oncogenes, are altered by mutations. They are directly responsible for neoplastic transformation. A single copy of a mutated gene leads to an activated oncogene, which is characterized by a dominant phenotype.

▪ **Tumor suppressor genes**: also known as oncosuppressors, are normal genes that slow down cell division, repair DNA mistakes, or tell a cell when to die. Oncosuppressors are recessive genes, making it necessary for mutation to occur on both alleles.

In general, mutations are required in both oncogenes and oncosuppressors in order for cancer to develop. A mutation limited to one oncogene would be eliminated by normal mitosis control processes and tumor suppressor genes. A mutation of a single tumor suppressor gene would also be insufficient to cause cancer due to the presence of a number of "backup copies" which duplicate its function. It is only when a sufficient number of proto-oncogenes and tumor suppressor genes mutate that allows uncontrolled cell growth to develop into a tumor.

▪ **Mutated genes**: Mutations result from damages to DNA which are not repaired, errors in the process of replication, or from the insertion or deletion of segments of DNA by mobile genetic elements. Mutations may or may not produce discernible changes in the observable characteristics (phenotype) of an organism. Mutations play a part in both normal and abnormal biological processes including evolution, cancer, and the development of the immune system, including junctional adversity. Therefore, the

expression of mutated genes depends on the mechanism and cellular “intent” of the mutation.

There are several factors, which can predispose and individual to cancer including cigarette smoke, air pollution, excessive consumption of alcohol, a sedentary lifestyle, physical and chemical agents and viruses.

Cancer can strike at any age, although advanced age can increase the probability of its occurrence due to the accumulation of damage and cellular mutations generated over time. Race, sex, hormonal imbalances and genetic predisposition to mutations are intrinsic factors that are transmitted from parent to child and cannot be controlled. Conversely, extrinsic factors are those related to external exposure to carcinogens. The primary extrinsic factors are ultraviolet and ionizing radiations. The first ones, derived from solar radiation or artificial sources, can cause mutations in the DNA of specific target cells: inactivation of enzymes, abnormal cell division, cell necrosis and cancer. The second ones increase the risk of solid tumors, especially in the lungs, and leukemia.

They can perform two actions:

- Direct toxic action: absorption of radiation by cells which causes the rupture of one or both strands of DNA resulting in cell death or mutation.
- Toxic indirect action: radiation energy is transferred to the water within a cell, promoting the formation of free radicals, which results in oxidative damage.

Tumors are classified as benign or malignant. Benign tumors are recognized by a slow, progressive growth, which does not invaded nearby or distant tissues; they are not very aggressive, they are delimited by a fibrous capsule (i.e. polyps, cysts, adenomas) and generally do not endanger the life of an individual. On the other hand, malignant tumors, are characterized by rapid growth, the ability to invade surrounding tissues and spread to distant tissues and structures. This process is called metastasis, which involves the migration of cancer cells through the blood and/or lymphatic system to anatomical sites distant from the origin to create secondary tumors. Therefore, they are very aggressive and can cause death if not treated in the early stages (i.e. cancer, carcinoma, sarcoma).

1.1 ANTICANCER THERAPY

Cancer is the second leading cause of death in developed countries after cardiovascular disease. Therapeutic treatments are divided as follows:

- **Surgery**: primary option for most solid tumors. Sometimes, radiation and/or chemotherapy is used preoperatively in an attempt to reduce the size of a tumor, in order to facilitate its removal.
- **Radiotherapy**: high power radiation to kill cancer cells. Generally, it is concentrated as much as possible in the affected site to prevent damage to healthy cells.
- **Chemotherapy**: cytotoxic drugs (toxic to cells). In general, it is used to block cell division in rapid replication, without, however, distinguishing between healthy and diseased cells. For this reason, chemotherapy produces side effects to all tissues with rapid cell turnover, such as mucous membranes, hair and blood. Usually, additional antineoplastic agents are administered through polychemotherapy. The primary purpose of polychemotherapy is to prevent drug-resistance in the neoplastic population. Moreover, the efficacy of a combination of drugs is generally higher than the sum of the effects of individual agents used in monotherapy due to a synergism. This promotes the same results with lower doses and, consequently, fewer side toxic effects for the organism. This is particularly important for antineoplastic drugs, which have a low therapeutic index.

1.2 ANTITUMORAL DRUGS

The common mechanism of action of antitumoral drugs is to prevent the growth and division of cancer cells or, at best, completely eliminate the tumor itself. The majority of antineoplastic drugs act specifically on processes such as DNA synthesis or assembly of the mitotic spindle. Others block the synthesis of DNA precursors or damage the integrity of the DNA and prevent transcription.

The growth and division of normal and neoplastic cells follows a sequence of events called the cell cycle, which is divided into different stages (**Figure 1**). Each stage is crucial for cell survival, but DNA synthesis and the formation of the mitotic spindle are the most

fragile. Cytotoxic drugs are historically classified as phase specific or phase-non-specific - intercalating agents or antibiotics, respectively - depending on their capacity to act only on cells undergoing replication or quiescent cells.

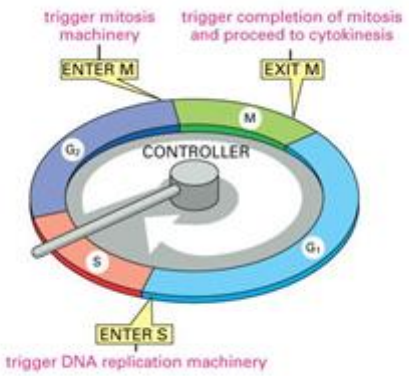

Figure 1. Cell cycle

Phase-specific drugs may exhibit selectivity for a specific phase of the cell cycle (for example: antimetabolites for the S-phase and vinca alkaloids for the M-phase). Phase-non-specific drugs are active in any phase of the cell cycle and they have a linear dose-response curve, that is, the greater the dose of drug, the greater is the fraction of cell kill. The major classes of anticancer drugs used in therapy are [3]:

- **Alkylating agents**: compounds with anticancer activity that act by inhibiting DNA replication and, secondarily, by inducing alterations in RNA transcription and blocking protein synthesis. They are defined as molecules able to insert alkyl groups in the nucleobases (usually at the N7 position of guanine). This alkylation process results in the formation of cross-links in the double helix: the adducts thus generated are then involved in a complex series of changes, variable depending on the compound used, which results in inhibition or inaccurate replication of DNA itself. Since they interact with DNA, proteins and RNA preformed, alkylating agents are phase-non-specific and therefore unable to discriminate between normal and tumoral DNA. As they act in a non-specific way, these agents have a low therapeutic index and important risk of toxicity. As an example, the alkylating agent EMS (*ethylmethane sulfonate)* donate an ethyl group to the keto group of guanine (**Figure 2**).

- **Antimetabolites**: they act specifically on the components of nucleobases of DNA. In particular, they interfere with the reactions leading to the ring formation of the purine or pyrimidine. Antimetabolites can interfere with the formation of these components, acting as antagonists to them (or antimetabolites). In this case, unlike the alkylating agents, it is important the exposure time: an higher exposure increase the number of molecules that will react.

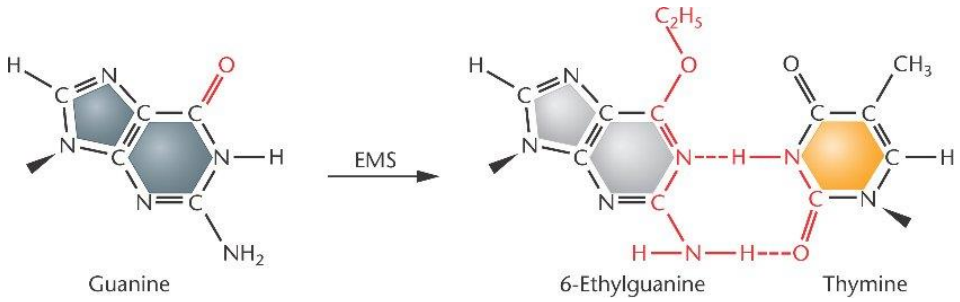

Figure 2. Ethylmethane sulfonate (EMS, a mustard gas) is an alkylating agent that can donate an alkyl group (C2H5) to a keto group in guanine.

- **Antimitotic drugs**: they work during the stage of cell division (mitosis), in particular at the stage where the newly synthesized DNA is shared between two daughter cells. The distribution of genetic material between cells is accomplished through the mitotic spindle, a complex structure made up of special proteins called microtubules. These drugs destroy or alter spindle formation, thus preventing cell replication and leading to the death of the cell (vinca alkaloids).
- **Intercalating agents**: they insert between two contiguous nucleobases along the strands of the double helix, when the cell begins its replicative cycle using DNA polymerases to insert a nucleotide along with the intercalating agent. This mechanism interrupts the replication cycle by preventing duplication of identical DNA strands.
- **Groove binders**: chemical compounds with oligopeptide side chains that bind to the major or minor groove of DNA.
- **Strand break**: they generate radical species that react with the saccharide portions causing rupture of the polynucleotide strand.

- **Topoisomerase Inhibitors**: they insert at the interface of the binary complex formed by DNA and the enzyme, inhibiting specifically the reformation stage of the chopped strand DNA.

Intercalating agents and the groove binders create reversible, non-covalent bonds with DNA. Alkylating agents and the strand break create irreversible bonds with DNA.

2. TOPOISOMERASES

DNA chromosomes are often longer than the cells in which they are contained. For this reason, DNA must be compacted requiring a high degree of structural organization. The folding mechanism compacts the DNA in a manner, which allows access to its information to conduct to processes such as replication and transcription. Two DNA strands, wrapped in a double helix, rotate around its own axis, which then folds back on itself causing a supercoiling of the DNA. Supercoiling can be positive, when the DNA is wrapped more than normal, and negative, when partially uncoiled. It affects many aspects of the metabolism of DNA. In every cell there are enzymes called topoisomerases which function to coil or uncoil DNA.

DNA topoisomerases are a diverse set of essential enzymes responsible for maintaining chromosomes in an appropriate topological state. All topoisomerases can harness the free energy stored in supercoiled DNA to drive their reactions. Some further use the energy of ATP to alter the topology of DNA away from an enzyme-free equilibrium ground state. In the cell, topoisomerases regulate DNA supercoiling and unlink tangled nucleic acid strands to actively maintain chromosomes in a topological state commensurate with particular replicative and transcriptional needs. To carry out these reactions, topoisomerases rely on dynamic macromolecular contacts that alternate between associated and dissociated states throughout the catalytic cycle [4].

All cells contain two major forms of topoisomerases, type I, which makes single-stranded cuts in DNA, and type II, which cuts and passes double-stranded DNA. Type I topoisomerases are further subdivided into two mechanistically distinct subgroups: type IA enzymes, which are homologous to E. coli topoisomerase I, and type IB enzymes, which are homologous to human topoisomerase I (**Figure 3**)[5].

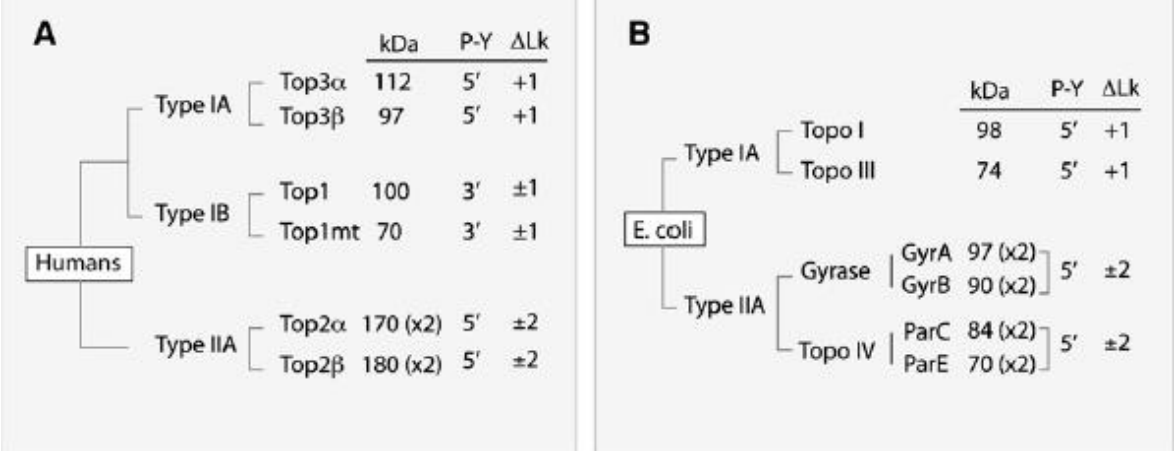

Figure 3. Classification of human (A) and *E. coli* (B) DNA topoisomerases

Topoisomerases play critical roles in DNA replication, transcription, and chromosome structure by altering the topological state of DNA. These enzymes are capable of relaxing supercoiled DNA and of decatenating interlocked DNA. While bacterial DNA gyrase, a type II topoisomerase, can introduce negative supercoils into DNA, all known eukaryotic topoisomerases can only relax DNA. The decatenation of interlocked DNA is a critical topoisomerase function, since semi-conservative DNA replication results in catenated sister chromatids (**Figure 4**).

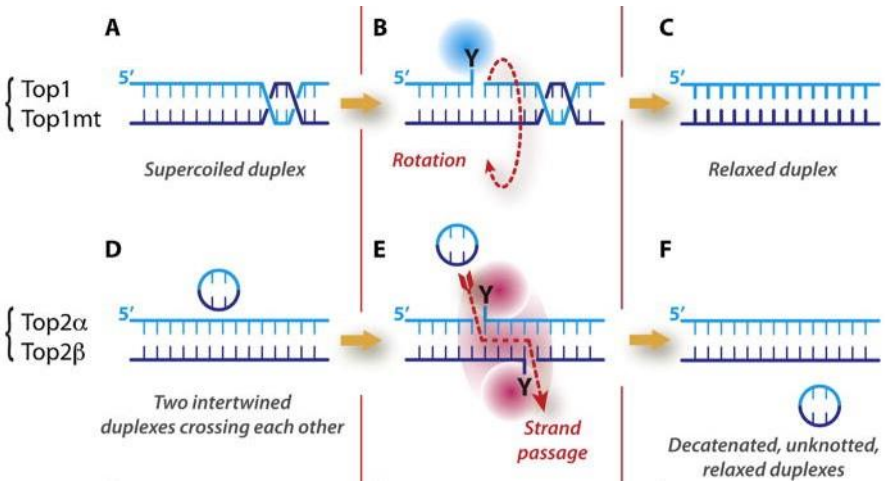

Figure 4. Mechanisms of action of topoisomerases and schematic representation of the cleavage complexes. (A)–(C) Topoisomerases I (Top1 for nuclear DNA and Top1mt for mitochondrial DNA) relax supercoiled DNA (A) by reversibly cleaving one DNA strand, forming a covalent bond between the enzyme catalytic tyrosine and the 3′ end of the nicked DNA (the Top1 cleavage complex: Top1cc; (B) This reaction allows the swiveling of the broken strand around the intact strand. Rapid religation allows the dissociation of Top1. (D)–(F) Topoisomerases II (Top2α and Top2β) act on two DNA duplexes (D) They act as homodimers, cleaving both strand, forming a covalent bond between their catalytic tyrosine and the 5′ end of the DNA break (Top2cc; (E)). This reaction allows the passage of the intact duplex through the Top2 homodimer (red dotted arrow; (E)). Religation and ATP hydrolysis allow the dissociation of Top2 (F).

2.1 TOPOISOMERASE 1 (Top1)

Topoisomerase I (Top1) is an abundant and essential enzyme. Top1 proteins belong to the family of the tyrosine recombinases (which includes λ-integrase, Flip and C-recombinases). Topoisomerases and tyrosine recombinases nick and religate DNA by forming a covalent enzyme-DNA intermediate between an enzyme catalytic tyrosine residue and the end of the broken DNA. These covalent intermediates are generally referred to as "**cleavage (or cleavable) complexes**", called **Top1cc** [6].

Biochemical and x-ray crystallographic data reveal an unusual architecture of monomeric Top1 (**Figure 5**).

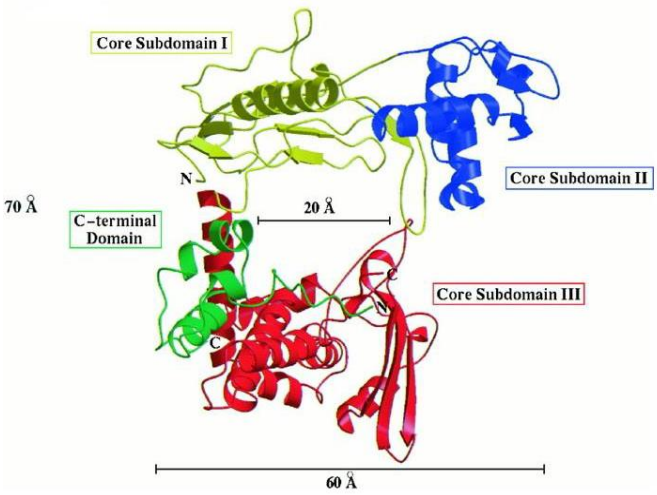

Figure 5. Structure of human Top1.

Top1 is a 765-aa (91-kDa) enzyme that catalyzes the relaxation of both negative and positive supercoils in a reaction that does not depend on an energy-rich cofactor or divalent cations. Based on limited proteolysis studies and the crystal structure, the protein can be divided into four discrete domains. The N-terminal domain, comprising approximately the first quarter of the protein, is highly charged and poorly conserved. This region of the protein is dispensable for enzymatic activity because a truncated form of the protein missing the first 174 aa (topo70) displays the same DNA relaxation activity as the full length protein *in vitro*. The remainder of the protein consists of the highly conserved core domain (54 kDa), the conserved C-terminal domain (8 kDa), which contains the nucleophilic tyrosine at position 723, and the poorly conserved and positively charged linker region (5 kDa) that connects the C-terminal domain to the core.

In addition to tyrosine 723 located in the C-terminal domain, the active site is composed of residues found in the core domain of the enzyme.

Based on the crystal structure, Top1 is a bi-lobed protein that clamps completely around duplex DNA through protein–DNA phosphate interactions. The core domain of the protein can be further divided into subdomains I, II, and III. One lobe of the protein, termed the cap region, consists of core subdomains I and II and sits on top of the duplex. It is composed of mixed α and β secondary structural elements and contains two unique nose-cone helices (α5 and α6) that extend 25 Å from the body of the molecule. The second lobe (core subdomain III, the linker, and the C-terminal domain) sits below the DNA, is composed of an all α-helical structure except for one three-stranded β sheet, and contains the catalytic residues implicated in the strand cleavage and religation reactions. In the closed clamp configuration found in the cocrystal structure, the two lobes are covalently joined through a continuous α-helical chain (α8) on one side of the DNA molecule, and contact each other in the "lips" region on the opposite side of the DNA, through the formation of a salt bridge between loops that extend from each of the lobes (**Figure 6**) [7].

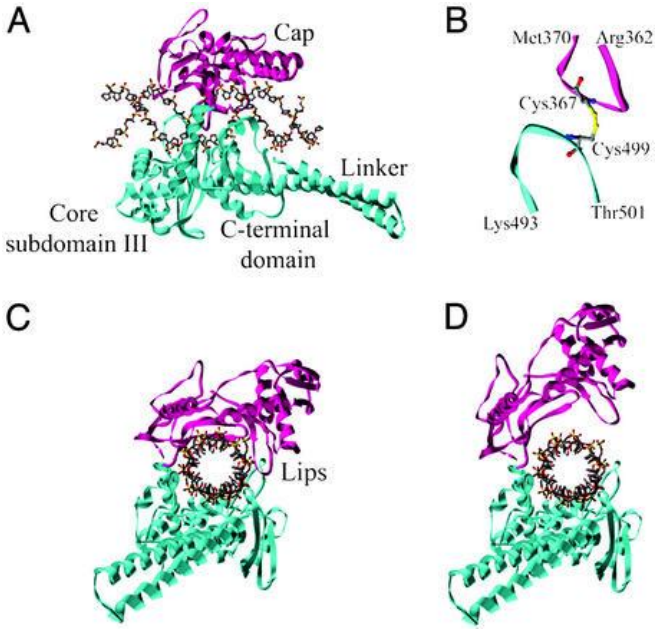

Figure 6. Schematic showing the key structural features of human topoisomerase I. (*A*) The crystal structure of human topoisomerase I (residues 215–765) in complex with a 22-bp DNA. Core subdomains I and II form the upper lobe or cap of the enzyme (magenta) and contain the nose cone helices. The lower lobe of the enzyme, shown in cyan, comprises subdomain III, the linker region, and the C-terminal domain. (*B*) The predicted structure for the disulfide bond formed between Cys-367 and Cys-499 in topo70^{2XCys}. The predicted distance between the Cβ atoms of the two cysteines is 4.6 Å. The two loops (Arg-362–Met-370 and Lys-493–Thr-501) follow the same color scheme as in *A*. (*C*) An end view of the cocrystal structure of human topoisomerase I looking down the axis of the DNA helix. The two opposing loops shown in *B* contact each other in a region referred to as "lips." (*D*) Model of a hypothetical open clamp form of the protein.

Activity of human Top1 involves four steps (**Figure 7)**:

1. DNA bond: the enzyme in the open conformation of its core domain recognizes the ribonucleotidic chain and leads to the subsequent formation of the non-covalent DNA-topoisomerase complex, Top1cc; this bond culminates in the closure of Top1 around nucleic acid, so that the subdomains I and III of the core domain are touching.
2. DNA cleavage: the amino acids of the active site are located in a position that prevent the nucleophilic attack by 723Tyr on phosphodiester bond of the DNA, to form a phosphotyrosinic bond and constitute the Top1 cleavage complexes.
3. DNA relaxation: the enzyme undergoes a conformational change, which allows the passage of the intact filament through the interruption produced in the other one.
4. DNA mending: it occurs by transesterification. Hydroxyl in 5' end of cleaved strand attacks the phosphate, aligned with the hydroxyl group itself, still bound to enzyme tyrosine within the complex Top1-Tyr-DNA. Thus, the original phosphodiester bond is reconstituted. Finally, the enzyme releases DNA [6,8].

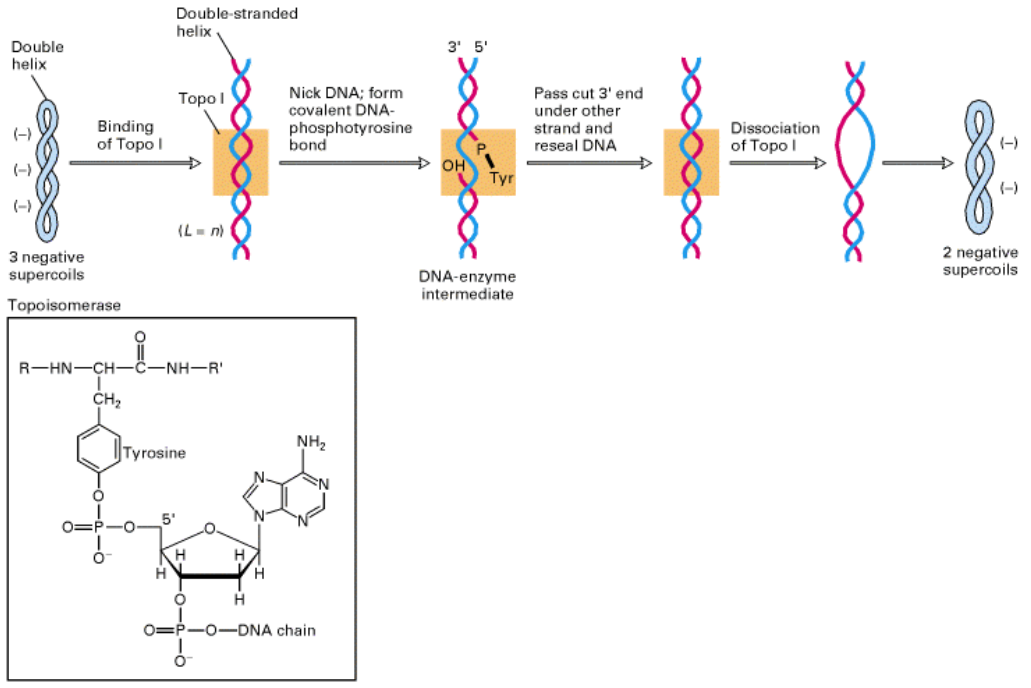

Figure 7. Mechanism of action of Topoisomerase I.

2.2 TOPOISOMERASE II (Top 2)

Type II DNA topoisomerases (Top2) catalyse the transport of one DNA double helix through another, in an ATP-dependent reaction. This manoeuvre allows the control of chromosomal DNA supercoiling, and the removal of DNA supercoils, knots and catenaes generated in a variety of biological processes including DNA replication, transcription and recombination. Type II enzymes are ubiquitous in nature, are biologically essential and share structural and evolutionary features. All type II topoisomerases require divalent metal ions for catalytic function. These metal ions function in two separate active sites and are necessary for the ATPase and DNA cleavage/ligation activities of the enzymes. ATPase activity is required for the strand passage process and utilizes the metal-dependent binding and hydrolysis of ATP to drive structural rearrangements in the protein (**Figure 8**).

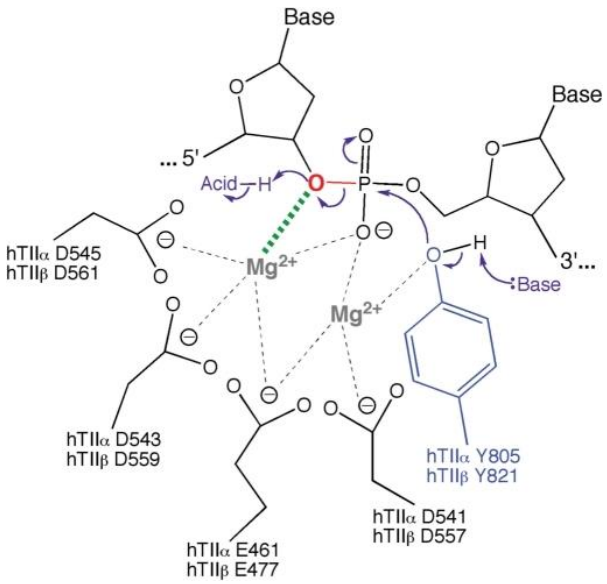

Figure 8. Mechanism of DNA cleavage and ligation mediated by topoisomerase II. The type II enzyme utilizes a two-metal ion mechanism similar to that utilized by primases and polymerases. Amino acids that are postulated to interact with the metal ions in the active site of topoisomerase IIα and topoisomerase IIβ are indicated. One of the metal ions (shown at left) makes a critical interaction with the 3′-bridging atom of the scissile phosphate (bond shown in red), which most likely is needed to stabilize the leaving 3′-oxygen (shown in red). A second metal ion (shown at right) is required for DNA scission and may stabilize the DNA transition state and/or help deprotonate the active site tyrosine (Y805 in topoisomerase IIα and Y821 in topoisomerase IIβ). Cleavage is initiated when a general base deprotonates the active site tyrosine hydroxyl, allowing the oxyanion to attack the scissile phosphate. The base has not been identified but is believed to be a conserved histidine residue. Ligation is initiated when a general acid extracts the hydrogen from the 3′-terminal hydroxyl group. The acid may be a water molecule or an unidentified amino acid in the active site of topoisomerase II

Topoisomerase IV and gyrase are the topoisomerases II enzymes expressed in bacteria. Topo IV mediates the unlinking of daughter chromosomes before cell division, whereas

gyrase is unique in its ability to introduce negative supercoils into DNA, thereby controlling chromosome supercoiling, which promotes replication fork advance and allows global regulation of gene expression. In each case, the active complex is a tetramer of two topo IV, ParC and ParE subunits, or gyrase, GyrA and GyrB proteins. The ParC and GyrA subunits have an N-terminal DNA breakage-reunion domain linked to divergent C-terminal β-pinwheel domains that favour intermolecular DNA passage by topo IV, causing DNA unlinking, but intramolecular DNA transport by gyrase, producing supercoiled DNA. By contrast, the N-terminal and C-terminal regions of the highly conserved ParE (GyrB) subunits form the ATPase- and Mg^{2+}-binding-TOPRIM domains, respectively. These four functional domains are also present in eukaryotic topo II but contained within each subunit of the homodimeric complex organized in a 'GyrB-GyrA' arrangement, i.e. N-terminal ATPase-TOPRIM-breakage/reunion-C-terminal domain. Thus, different Top2 share close functional and architectural similarities (**Figure 9**) [9].

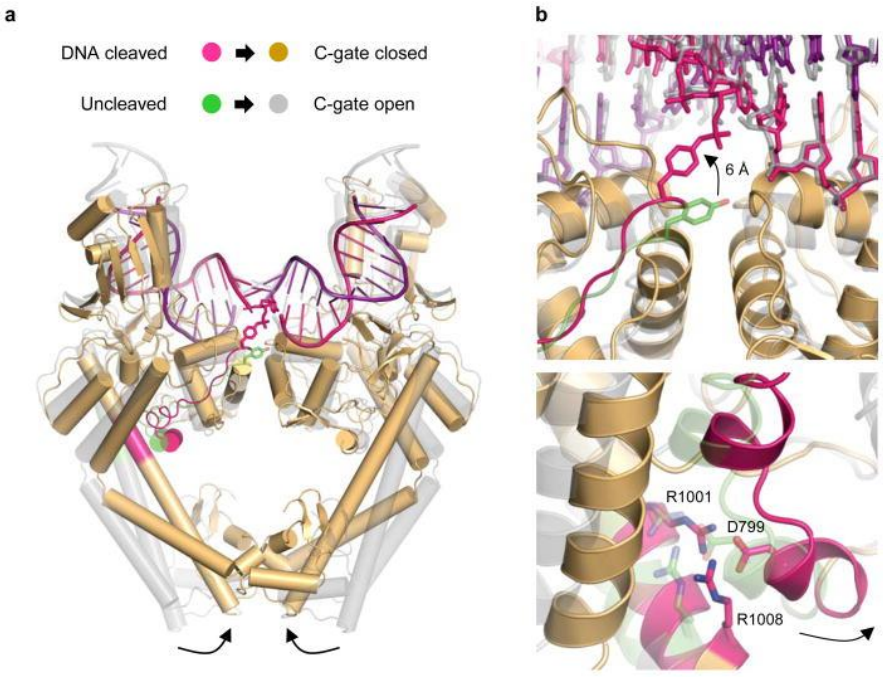

Figure 9. Cleavage-dependent control of C-gate dynamics. **a.** Superposition of noncovalent (grey) and cleavage (orange) complexes between topo II and DNA reveal how C-gate opening and closure is linked to active site status. The connection from the active-site tyrosines to the coiled-coil arms is coloured green/magenta. For clarity, the TOPRIM domains are hidden. **b.** Close-up of positional shifts. (*Upper*) Upward movement of the active-site tyrosine upon becoming attached to the DNA. (*Lower*) Concomitant inward movement of the coiled-coil joint through a conserved salt bridge network.

Structural and biochemical studies, particularly on gyrase and yeast topo II, have led to the formulation of a general mechanistic model for Top2. The enzymes operate as symmetrical dimers; the eukaryotic proteins are homodimers, while the bacterial

homologues divide the polypeptide into two distinct gene products and are A_2B_2 tetramers. Both classes of Top2 interact with two DNA segments. The G- (or 'Gate'-) segment first binds to and is strongly bent by the enzyme. Each strand of this DNA is then cleaved by one of a pair of tyrosines forming two covalent 5'-phosphotyrosine intermediates. ATP binding to each monomer results in dimerization of the N-terminal domains to form a new protein–protein interface (termed the N-gate), enclosing a second DNA (the T- or 'Transported'-segment), which is passed through the G-segment; this process requires not only DNA cleavage, but also the separation of the DNA ends by disruption of an existing protein dimer interface (the DNA gate). The T-segment subsequently leaves the complex through a third protein interface (the C- or exit-gate), having passed through the G-segment and across the entire dimer interface of the enzyme. ATP hydrolysis and product release allows the N-gate to open and resets the enzyme for further rounds of reaction, although hydrolysis of one ATP and release of phosphate also appears to stimulate strand passage (**Figure 10**) [10].

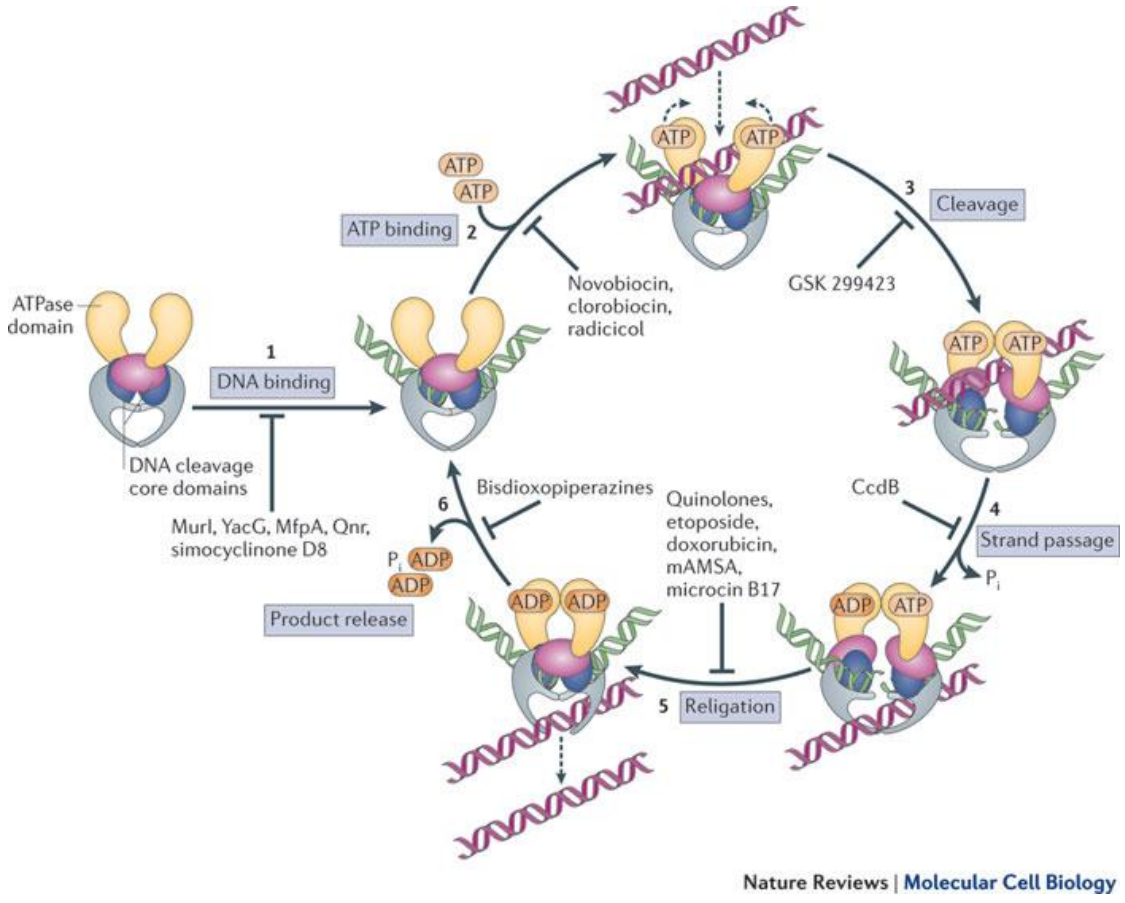

Figure 10. Structure and mechanism of Top2**.** The Top2 reaction cycle and all of the points at which exogenous agents can disrupt function. During catalysis, the topoisomerase initially binds one duplex DNA segment (step 1). Following binding, the topoisomerase can then associate with a second duplex DNA segment. ATP binding (step 2) stimulates cleavage and opening of the first DNA (step 3), and passage of the second through the opening (step 4). The broken strands are then religated (step 5), and the product is released (step 6). Agents have been identified that interfere with each step, as indicated, but only a partial list of inhibitors and poisons is given here. mAMSA, amsacrine; MurI, glutamate racemase.

3. TOPOISOMERASE 1 INHIBITORS

Nuclear DNA topoisomerase I (Top1) is an essential human enzyme. It is the only known target of the alkaloid camptothecin, from which the potent anticancer agents irinotecan and topotecan are derived. As camptothecins bind at the interface of the Top1-DNA complex, they represent a paradigm for interfacial inhibitors that reversibly trap macromolecular complexes. Several camptothecin and non-camptothecin derivatives are being developed to further increase anti-tumour activity and reduce side effects. The mechanisms and molecular determinants of tumour response to Top1 inhibitors are reviewed, and rational combinations of Top1 inhibitors with other drugs are considered, based on current knowledge of repair and checkpoint pathways that are associated with Top1-mediated DNA damage [11].

Anticancer Top1 inhibitors act by slowing down the reversal of Top1cc and religation of DNA. Persistence of Top1cc leads to collisions with replication forks and transcription complexes, converting them into irreversible Top1 covalent complexes and DNA double-strand breaks, which, if not repaired, are lethal. The anticancer activity of Top1 inhibitors is primarily related to replication damage by replication “run-off” and replication-mediated DNA double-strand breaks (**Figure 11**) [12].

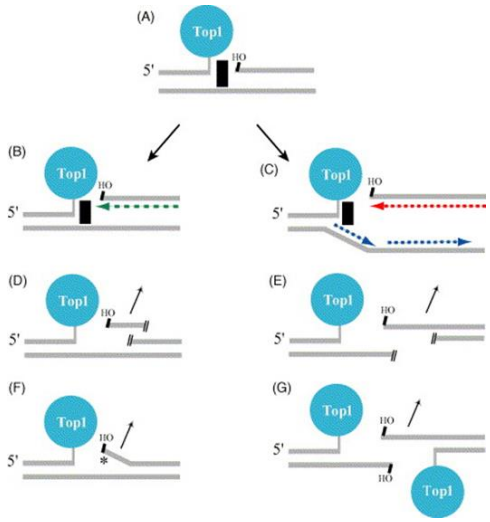

Fig. 11. Conversion of Top1 cleavage complexes into DNA damage by displacement of the 5′-hydroxyl at the end of the cleaved strand by DNA replication, transcription, or preexisting DNA lesions. (A) Schematic representation of a Top1 cleavage complex trapped by camptothecin (black rectangle). Top1 is covalently bound to the 3′-end of the broken DNA. The other end is a 5′-hydroxyl. (B) Conversion of the cleavage complex into a covalent Top1–DNA complex by a colliding transcription complex (the RNA is shown in green). (C) Conversion of the cleavage complex on the leading strand into a covalent Top1–DNA complex by a colliding replication fork (the leading replication is shown in red; the lagging replication in blue). (D and E) Formation of a suicide complex by a single-strand break on the same (D) or the opposite (E) strand from the Top1 scissile strand. (F) Formation of an irreversible Top1cc by a base lesion ((∗) abasic site, mismatch, oxidized base) at the 5′-end of the cleavage site. (G) Formation of a double-strand break at two Top1 cleavage sites close to each other.

Camptothecin (**CPT**) is a plant alkaloid first identified from the Chinese tree, *Camptotheca acuminata* (**Figure 12**). Soon after the discovery that CPT inhibited Top1 by trapping Top1cc, three lines of evidence demonstrated the selective poisoning of Top1 by CPT:

1) only the natural CPT isomer was active against Top1;
2) genetically modified yeast deleted for Top1 (*Top1*Δ) was immune to CPT;
3) cells, selected for CPT –resistance, showed point mutations in the Top1 gene.

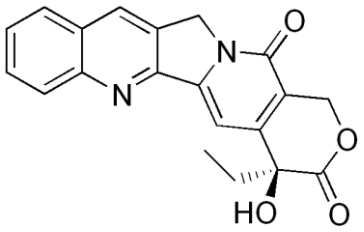

Figure 12. Camptothecin structure

CPT suffers from many limitations including poor stability and solubility. To overcome the solubility and stability issues associated with CPT, various derivatives have been developed.

Two water-soluble CPT derivatives are presently approved by the FDA for IV administration: topotecan and irinotecan (**Figures 13-14**).

Topotecan (Hycamtin®, **Figure 13**) is used to treat ovarian cancers and small-cell lung cancers (SCLC). However, hematological toxicity is a common side effect due to the destruction of bone marrow progenitors. As a result, infections can occur due to loss of white blood cells, bruising or bleeding to the loss of platelets, and anemia with fatigue to loss of red blood cells. Within a day following infusion, patients generally feel sick with nausea and possibly vomiting, which can generally be controlled with anti-emetic drugs. Patients may also feel tired during the first weeks of treatment. Hair loss starts 3–4 weeks after the first dose. It is temporary. Hair re-grows once the treatment is finished. Because

of potential teratogenic effects, it is recommended to use contraception during topotecan treatment and a few months afterwards.

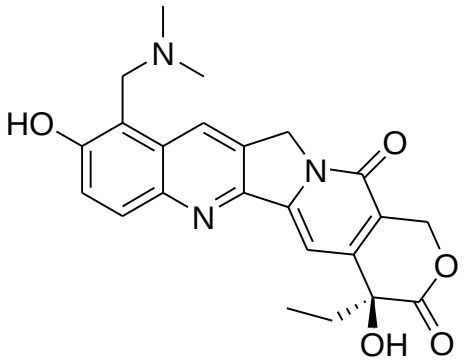

Figure 13. Topotecan structure.

Irinotecan (**Figure 14**) is approved by the FDA for colorectal tumors. It is a prodrug and needs to be converted to its active metabolite SN-38 by carboxylesterase. The most severe side effect is diarrhea, which can be severe. Temporary liver dysfunction is generally asymptomatic. The other side effects are the same as those produced by topotecan.

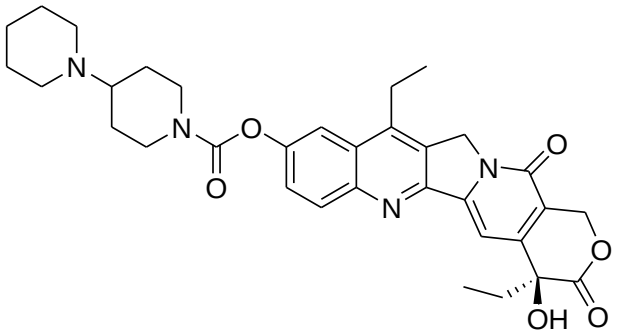

Figure 14. Irinotecan structure.

Two newer CPT derivatives are in clinical trials, Gimatecan and Belotecan. Both have shown some activity in glioma (**Figure 15**).

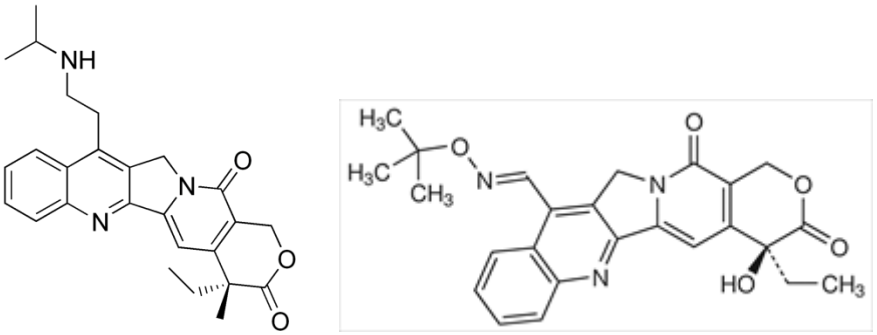

Belotecan **Gimatecan**

Figure 15.

One of the main limitations of all CPT derivatives is their spontaneous and rapid inactivation (within minutes) by E-ring opening. Although this reaction is potentially reversible, its equilibrium favours the carboxylate form at physiological neutral pH. Moreover, the active lactone derivatives is rapidly depleted in the blood stream due to the tight binding of the carboxylates to serum albumin (**Figure 16**).

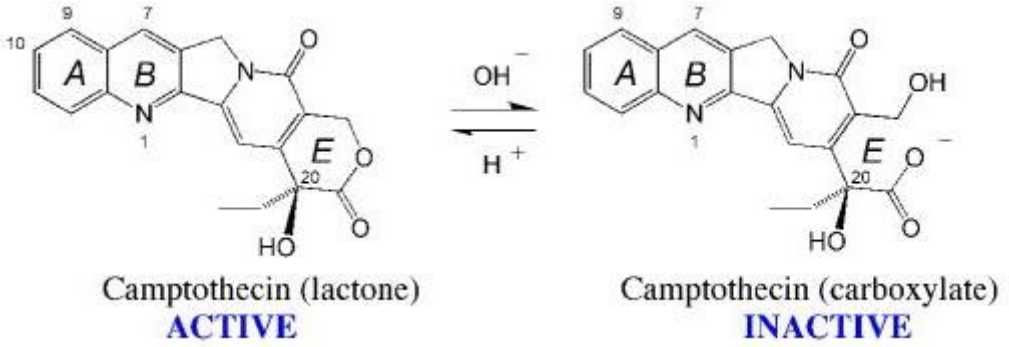

Figure 16. Camptothecin inactivation.

Two approaches have been taken to overcome the E-ring lactone instability. The first was to enlarge the E-ring by one carbon atom, which limits E-ring opening but also prohibits its reclosure. The corresponding compounds are synthetic and named **homocamptothecins**.

Diflomotecan is the clinical derivative (**Figure 17**). However, this approach is potentially problematic as irreversible E-ring opening inactivates homocamptothecin. From a chemical biology standpoint, one reason for studying the homocamptothecins was the presence of bound carboxylate in the crystal structure of topotecan, which is in contrast with the fact that the carboxylate form of CPT is clinically ineffective and inactive in

trapping Top1cc. Since homocamptothecin are at least as potent as CPT in spite of limited E-ring opening, this suggests that E-ring opening was not necessary for trapping Top1cc.

A second reason for studying homocamptothecins was to determine whether changing the E-ring could overcome the known drug efflux multidrug resistance mechanism to CPTs. Interestingly, we found limited impact of ABCG2 drug efflux resistance for homocamptothecins, which gives them an advantage over the CPTs.

The second approach to stabilize the E-ring was to convert the E-ring from a 6- to a 5-membered ring. Complete stabilization of the E-ring has been successfully achieved with the synthesis of the α-keto derivatives (exemplified by S39625). Removal of the lactone precludes E-ring opening (**Figure 17**).

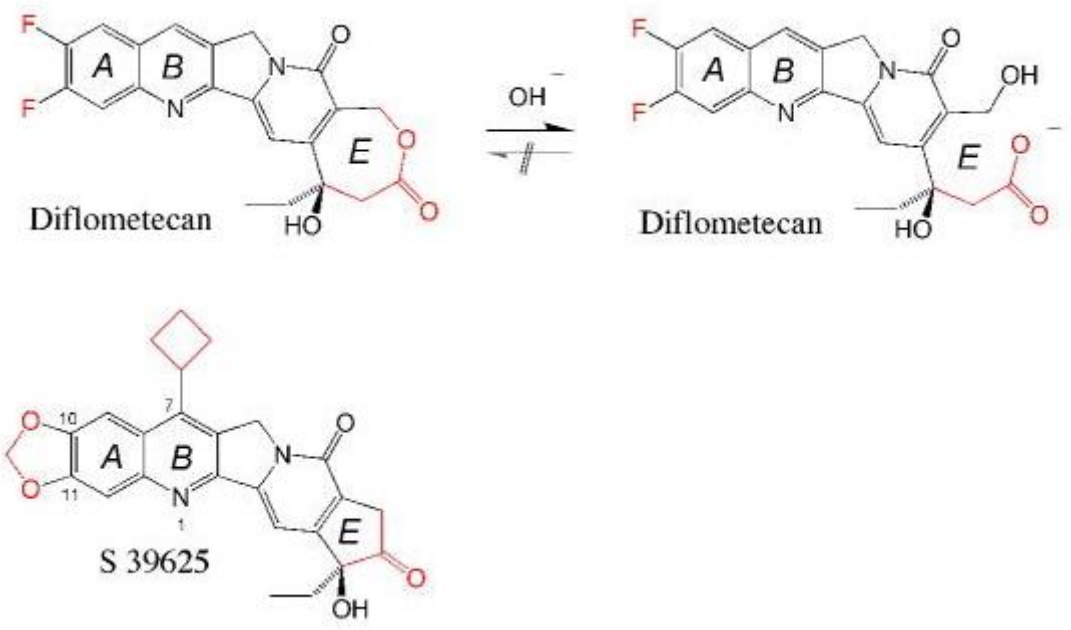

Figure 17. E-ring modified camptothecin derivatives in clinical trials.

This novel series provided a further test for the relationship between lack of E-ring opening and trapping of Top1cc. The remarkable potency of this novel drug class against purified Top1 and in cells, with selective targeting of Top1, and persistent Top1cc indicate the tight binding of S39625 to Top1cc (**Figure 17**). These experiments provide further evidence that lactone E-ring opening is not necessary for the trapping of Top1cc by CPT derivatives.

The indenoisoquinolines are one of the three classes of non-CPT Top1 inhibitors in clinical development. The selected indenoisoquinolines have several favorable characteristics (**Figure 18**):

1) They are chemically stable, which is not the case of CPTs;
2) They trap Top1cc at differential sites from CPTs, which is indicative of potentially different gene targeting;
3) Their anti-proliferative activity is similar to or greater than CPTs in the NCI60 cell lines;
4) They selectively target Top1 in cells, as demonstrated by high resistance of Top1-deficient P388 cells, and cross-resistance of cells with Top1-downregulation by shRNA;
5) They are not substrates of ABC membrane transporters, which suggest the ability to overcome resistance to CPTs;
6) Their antitumor activity in animal models is better correlated with effects on human bone marrow progenitors, suggesting that therapeutic doses in mice might be achievable in humans.

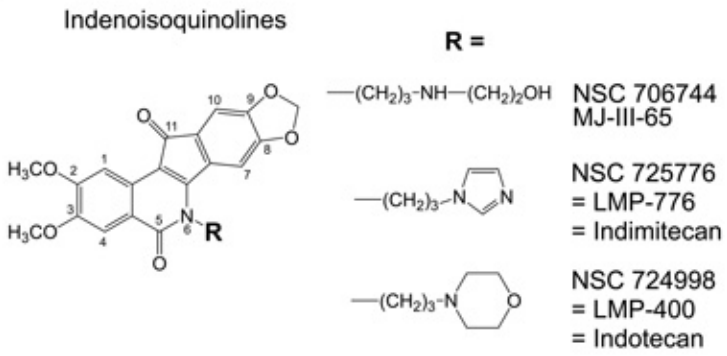

Figure 18. Indenoisoquinolines and its derivatives.

The indolocarbazoles were the first non-CPT derivatives introduced. Their current clinical development as anticancer drugs does not appear very active. More interesting are the phenanthridine derivatives. The phenanthridine derivatives (ARC-111) share many of the same advantages as the indenoisoquinolines, which is not surprising considering the chemical similarities between the indenoisoquinoline and phenanthridine families (**Figure 19**) [13].

Indolocarbazoles **Phenanthridine**

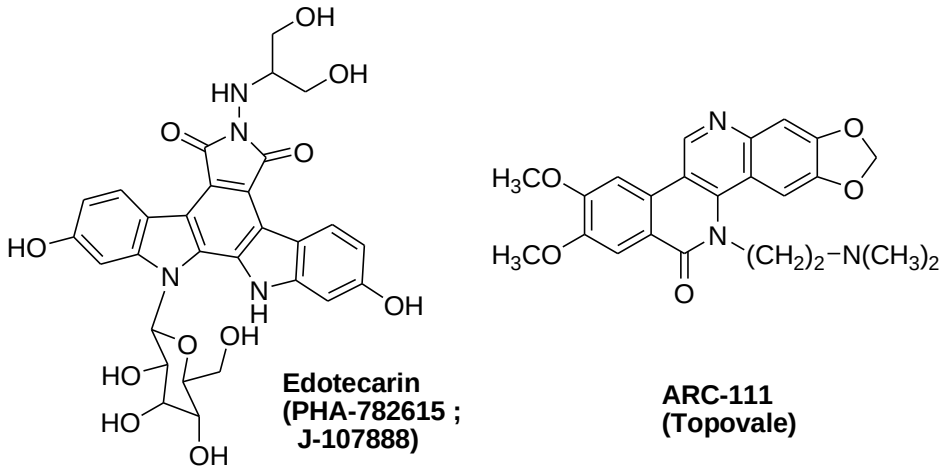

Edotecarin (PHA-782615 ; J-107888)

ARC-111 (Topovale)

Figure 19.

4. TOPOISOMERASE II INHIBITORS

Topoisomerase II (Top2) is inhibited by a variety of antitumor drugs, like **Doxorubicin**, **m-AMSA** (Amsacrine), **Epipodophyllotoxins**, and **Mitoxantrone**, that interfere with the breakage and religation of the G-segment of DNA, forming structures which favour DNA strand breakage often referred to as "cleavable complexes"(**Figure 20**).

In the absence of antitumor agents, such structures are usually short-lived. The presence of antitumor agents induces a large number of cleavable complexes, which if unresolved ultimately lead to cell death. **ICRF-159**, a Bisdioxopiperazine derivative which "locks" the ATP-operated clamp of the enzyme, and **Merbarone**, a thiobarbiturate derivative which acts via an yet unknown mechanism, also inhibit DNA topoisomerases and are cytotoxic agents.

In contrast to what is found for many other eukaryotes, there are two isoforms of human Top2, topoisomerase IIα and topoisomerase IIβ. Although it is known that both human isoenzymes can be inhibited by antitumor agents such as **Etoposide**, **m-AMSA**, and **Merbarone** *in vitro*, the extent to which inhibition of either topoisomerase IIα or IIβ is cytotoxic *in vivo* is unclear.

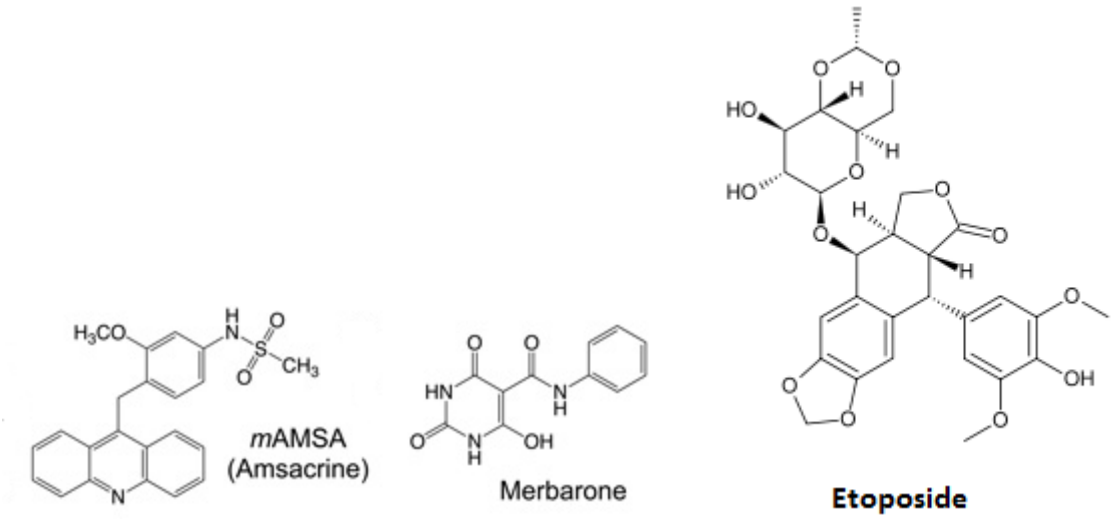

Figure 20. Topoisomerase II inhibitors.

Topoisomerase IIα is known to be preferentially expressed during mitosis, whereas topoisomerase IIβ shows little variation in levels during the cell cycle. One would speculate from these data that topoisomerase IIα is the major target of cytotoxic agents. However, drug-resistant cell lines have shown altered levels of either or both topoisomerase isoforms, suggesting some drug selectivity for α or β isoforms, and there have been some *in vitro* studies suggesting that α and β isoforms respond differently to different topoisomerase inhibitors. However, the exact nature of such selectivity was difficult to determine due to the problems associated with the isolation and separation of the two isoforms for both *in vivo* and *in vitro* studies [14].

5. TYROSYL-DNA PHOSPHODIESTERASE

Tyrosyl-DNA phosphodiesterases (TDP1 and TDP2) are among the most recently discovered DNA repair enzymes. They liberate DNA ends from the covalently stalled topoisomerase by cleaving the covalent phosphotyrosyl bond linking the topoisomerase to DNA, a process that is tightly regulated by post-translational protein modifications.

Eukaryotes possess two distinct TDPs as defined by their enzymatic activities *in vitro*. These are a metal independent TDP1, which primarily acts on DNA breaks with 3'-phosphotyrosyl termini, and a metal-dependent TDP2, which acts on DNA breaks with 5'-phosphotyrosyl termini. However, TDP2 also possesses weak 3'-TDP activity *in vitro* and,

in fact, was identified in a screen for novel TDP1-like activities that complement the sensitivity of TDP1-mutant budding yeast cells to Top1-induced DNA damage.

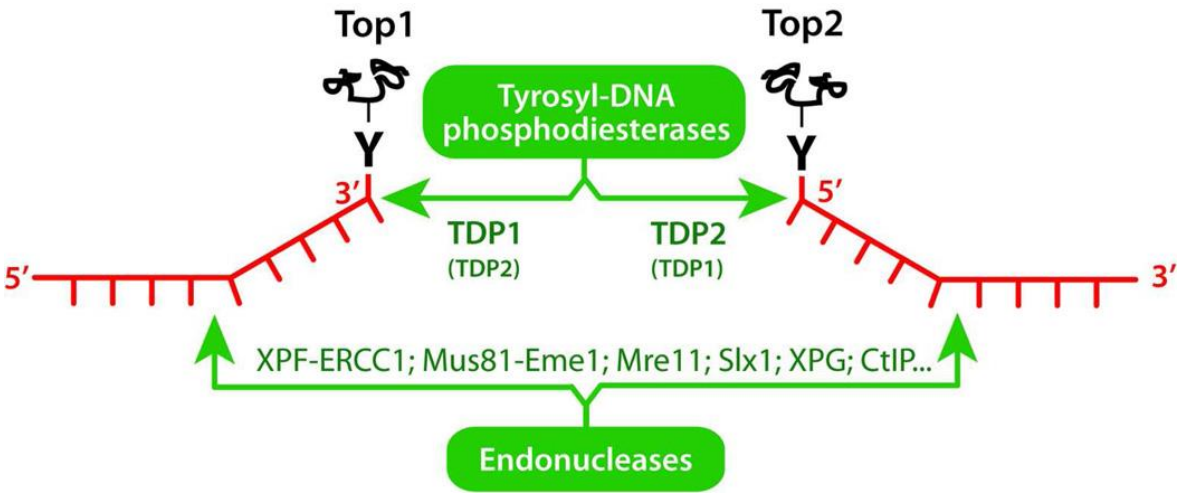

Figure 21. Schematic representation of the two main repair pathways removing topoisomerase-DNA complexes.

Both enzymes have an extended spectrum of activities. TDP1 not only excises trapped topoisomerases I (Top1 in the nucleus and Top1mt in mitochondria), but also repairs oxidative damage-induced 3′-phosphoglycolates and alkylation damage-induced DNA breaks, and excises chain terminating anticancer and antiviral nucleosides in the nucleus and mitochondria.

The repair function of TDP2 is devoted to the excision of topoisomerase II and potentially topoisomerases III-DNA adducts. TDP2 is also essential for the life cycle of picornaviruses (important human and bovine pathogens) as it unlinks VPg proteins from the 5′-end of the viral RNA genome [15].

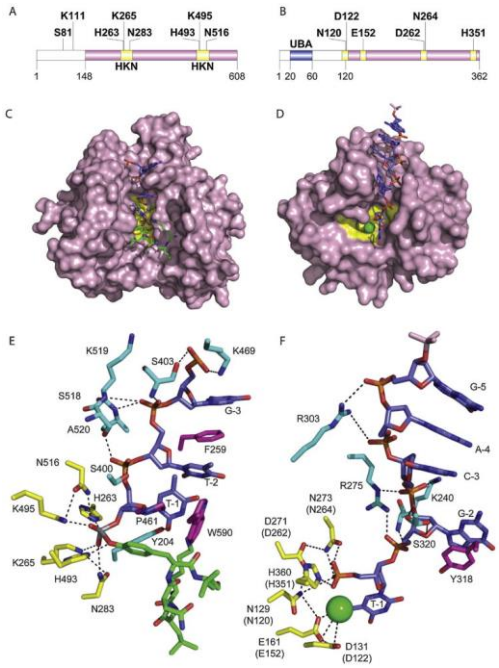

Figure 22. Crystal structures of TDP1 (left) and TDP2 (right). (A) and (B) Ribbon representation of TDP1 (A) and TDP2 (B) polypeptides. N-terminal (white) segments (residues 1–148 for TDP1 and 1–120 for TDP2) are absent in the crystal structures shown below. UBA in TDP2: ubiquitin binding associated domain. Conserved catalytic segments are highlighted in yellow. (C) and (D) Surface representations of the crystal structures for TDP1 ((C) PDB ID 1NOP) and TDP2 ((D) PDB ID 4F1H). Proteins are represented in light pink, catalytic residues in yellow, DNA in blue sticks, peptide in green sticks and both sticks colored by element (N, blue; O, red; P, orange; Vanadate, grey). For TDP2, magnesium is represented as the green sphere. (E) and (F) Detailed contacts between substrates and TDP residues in the catalytic site of TDP1 (E) and TDP2 (F). Catalytic residues are represented as yellow sticks; residues involved in polar interactions are in cyan sticks; residues involved in hydrophobic interactions in magenta sticks. All sticks are colored by element (N, blue; O, red; P, orange; Vanadate, grey). Dashed lines highlight polar interactions.

5.1 TYROSYL-DNA PHOSPHODIESTERASE 1 (TDP1)

Tyrosyl-DNA phosphodiesterase I (TDP1) is a member of the phospholipase D superfamily and hydrolyzes 3'phospho-DNA adducts via two conserved catalytic histidine and lysine residues within two conserved **HKD motifs**, one acting as the lead nucleophile and the second as a general acid/base. Althoug, TDP1 shares the conserved His and Lys residues in these two motifs, the Asp residue is not present, which places TDP1 in a novel subclass (HK-motif) within the PLD superfamily. Mechanistic and structural studies on human TDP1 (hTDP1) and yeast (*Saccharomyces cerevisiae*) TDP1 (yTDP1) have revealed that the conserved histidine residue in the first motif or the 'N-terminal histidine' (**His263** in hTDP1 and **His182** in yTDP1) functions as the lead nucleophile to cleave the 3' adduct from the DNA. The 'C-terminal histidine' within the second motif (**His493** in hTDP1 and **His432** in yTDP1) functions as a general acid/base to first protonate the leaving adduct, and then activate a water molecule for the second nucleophilic attack that resolves the TDP1-DNA covalent enzyme intermediate (**Figure 23**). Upon dissociation, TDP1 leaves a

single-strand break (SSB), and the 5’ and 3’ ends undergo further processing prior to religation by DNA ligase [16]. The resulting phosphoramide is stabilized by hydrogen-bonding with catalytic K265 and K495. Hydrolysis of this covalent intermediate occurs via a second SN2 reaction by a water molecule with the H493 residue acting as a general base. This proposed reaction step is supported by *in vitro* studies showing that the SCAN1 H493R mutation leads to an accumulation of TDP1-DNA covalent intermediate. The final product in this process is a DNA molecule with a 3’-phosphate end.

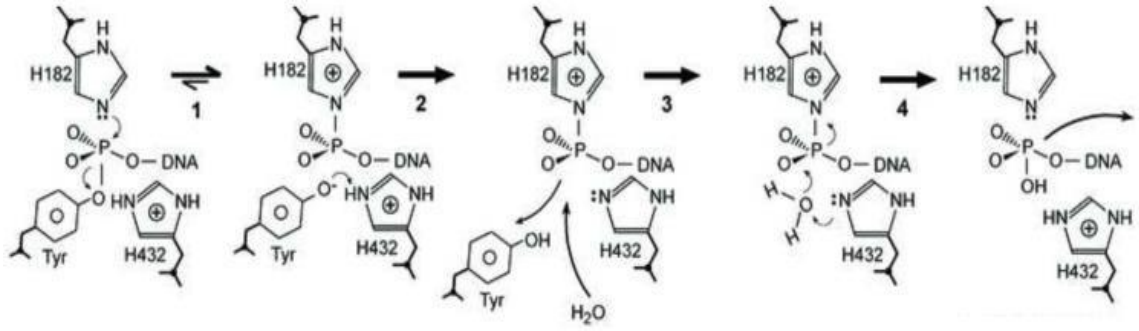

Figure 23. TDP1 catalytic mechanism. For simplicity, we only depict the catalytic His residues (yeast residue numbering) and the 3’phosphotyrosyl linkage as substrate. Step 1 can be reversed when the leaving phenoxyanion of Tyr is not protonated by the general acid His432, and reforms the original Top1-DNA intermediate. His432 subsequently functions as general base that activates water during step 3, and this results in dissociation of TDP1 from the DNA, which still contains a single strand nick.

TDP1 does not require nucleotide cofactor or metal. Yet, its catalytic mechanism is relatively complex, as TDP1 processes its substrates in two steps with a transient covalent intermediate.

The first step consists in a nucleophilic attack of the Top1-DNA phosphotyrosyl bond by H263 residue from the N-terminal HKN motif. The H493 residue from the opposite HKN motif acts as a general acid and donates a proton to the tyrosine containing peptide-leaving group. A transient covalent phosphoamide bond is formed between H263 and the 3’-end of the substrate. The opposite H493 residue acts as a general base, and hydrolyzes this covalent intermediate via an activated water molecule. This generates a product with a 3’-phosphate end, which needs to be further processed by polynucleotide kinase phosphatase (PNKP). Mutation of one of the catalytic histidines to an arginine residue at position 493 (H493R) results in the accumulation of covalent TDP1-DNA intermediates, ultimately leading to a rare autosomal recessive neurodegenerative disease called spinocerebellar ataxia with axonal neuropathy (SCAN1). As discussed above, wild-type

TDP1 can process this phosphoamide intermediate, which explains why SCAN1 patients have the H493R homozygous mutation (**Figure 24**) [15].

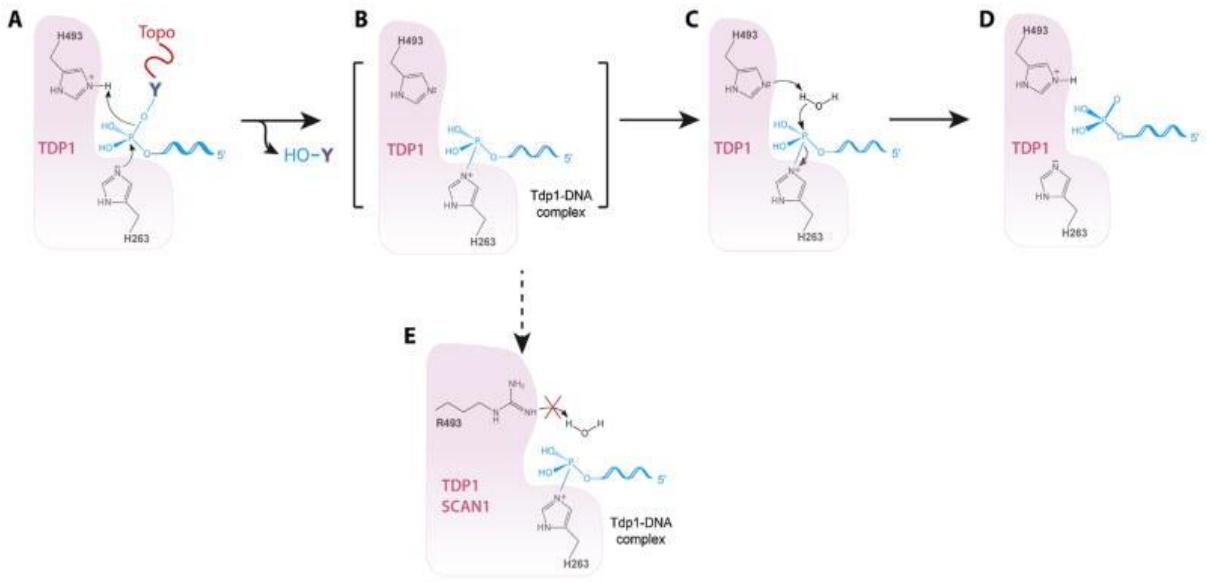

Figure 24. TDP1 catalytic cycle. (A) Nucleophilic attack of the phosphodiester backbone by the imidazole N2 atom of H263. H493 donates a proton to the tyrosyl moiety of the leaving group. (B) Phosphohistidine covalent intermediate. (C) Second nucleophilic attack via an activated water molecule by H493. (D): Generation of a final 3'-phosphate product and free TDP1. (E) The SCAN-1 mutations (H493R) leads to an accumulation of the TDP1-DNA intermediate and a defect in TDP1 turn- over rate.

In addition, a second group of conditional genes are the three sets of genes implicated in the structure-specific endonuclease repair pathways. *Rad1*/*Rad10* (*XPF*/*ERCC1*) functions primarily in the nucleotide excision repair pathway, where it cleaves on the 5'-side of the repair bubble formed around bulky DNA lesions. *Mus81*/*Mms4* (*Mus81*/*Eme1*) and *Mre11*/*Rad50*/*Xrs2* (*Mre11*/*Rad50*/*Nbs1*) cleave a 3'-flap upstream of a branch point and function independently from the TDP1 pathway. Mutations in each of these genes render *TDP1*-deficient yeast cells highly sensitive to CPT. Specific homologues for each of the genes mentioned above are present in humans with the exception of *Rad9* (**Figure 25**) [17].

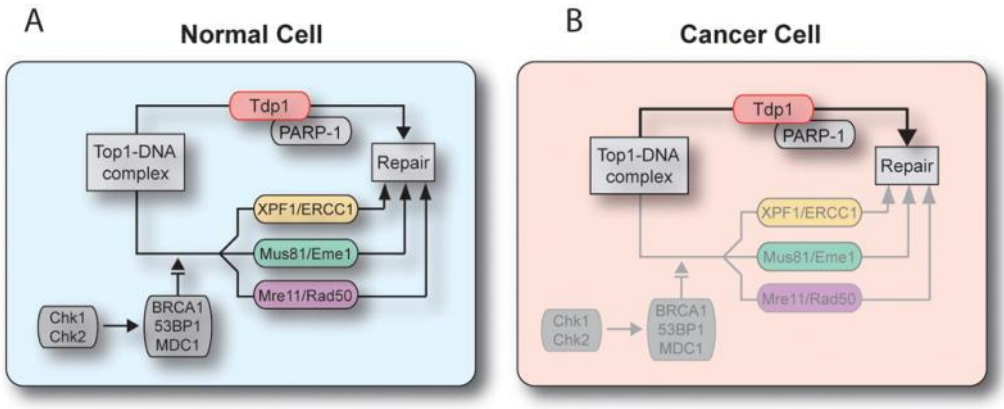

Figure 25. Rationale for TDP1 inhibitors:(A) In normal cells, Top1-DNA covalent complexes can be repaired by redundant mechanisms, which can be divided in two main pathways: i/the TDP1 hydrolysis pathway), and ii/the 3'-endonuclease pathway. (B) Cancer cells might be more dependent on the TDP1 pathway as a result of mutations and inactivation of DNA checkpoints (BRCA1, Chk2…). The expected effect of combining a TDP1 inhibitor with a Top1 inhibitor would be an increase in the therapeutic index of the Top1 inhibitor as the TDP1 inhibitor would sensitize preferentially the cancer cells.

5.2 TYROSYL-DNA PHOSPHODIESTERASE 1 INHIBITORS

Studies from SCAN1 cells provided evidence for TDP1 participation in the repair of Top1-mediated DNA damage and for the hypersensitivity to CPT in human cells with a single defect in TDP1 activity. These observations suggest the possibility of developing TDP1 inhibitors that can potentiate the cytotoxic effects of Top1 inhibitors in anticancer drug therapy.

To date, there are very few known TDP1 inhibitors, and their potencies and specificities leave much room for improvement. For example, both vanadate and tungstate can mimic the phosphate in the transition state, thus expressing inhibition at millimolar concentrations. However, due to poor specificity and hypersensitivity to all phosphoryl transfer reactions, they cannot serve as pharmacological inhibitors [18].

TDP1 inhibitors known so far are:

- **Aminoglycoside Antibiotics.** A recent study reports that neomycin inhibits TDP1 more effectively than the related aminoglycosides paromomycin and lividomycin A. Inhibition of TDP1 by neomycin is observed both with single- and double-stranded substrates, but is slightly stronger with duplex DNA, which is different from aclarubicin, which only inhibits TDP1 with the double-stranded substrate. Inhibition by neomycin can be overcome with excess TDP1 and is greatest at low pH. To our knowledge, aminoglycoside antibiotics and the ribosome inhibitors

thiostrepton, clindamycin-2-phosphate, and puromycin are the first reported pharmacological TDP1 inhibitors [19].

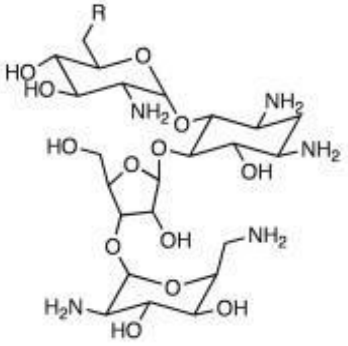

Neomycin B R=NH2
Paromomycin R=OH

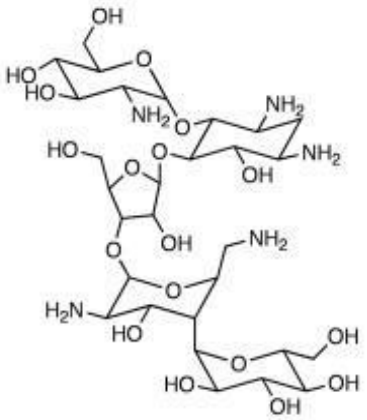

Lividomycin

- **Steroid derivatives.** Using a novel high-throughput screening assay, the C21-substituted progesterone derivative, NSC 88915, was identified as a potential TDP1 inhibitor. Secondary screening and cross-reactivity studies with related DNA processing enzymes confirmed that NSC 88915 (**Figure 26A**) possesses specific TDP1 inhibitory activity. Deconstruction of NSC 88915 into discrete functional groups reveals that both components are required for inhibition of TDP1 activity. Moreover, the synthesis of analogues of NSC 88915 has provided insight into the structural requirements for the inhibition of TDP1. Surface plasmon resonance shows that NSC 88915 binds to TDP1, whereas an inactive analogue fails to interact with the enzyme. Based on molecular docking and mechanistic studies, these compounds were proposed as competitive inhibitors, which mimics the oligonucleotide-peptide TDP1 substrate. These steroid derivatives represent a novel chemotype and provide a new scaffold for developing small molecule inhibitors of TDP1 [20].

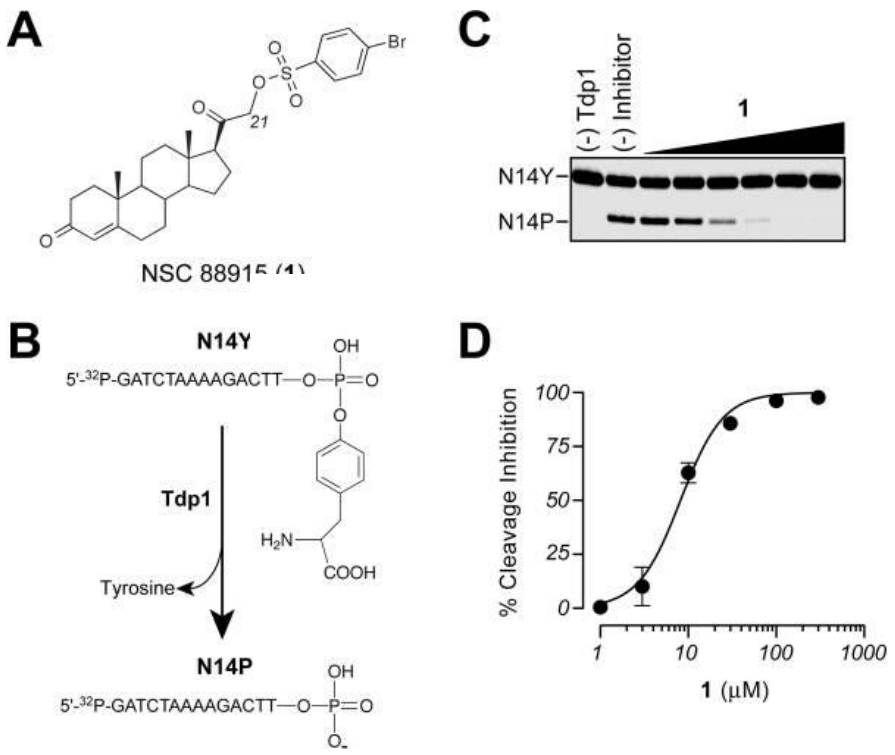

Figure 26. TDP1 inhibition by NSC 88915. A) Chemical structure of NSC 88915. B) Schematic representation of the TDP1 gel-based biochemical assay. TDP1 hydrolyzes the 3'-phosphotyrosine bond and converts N14Y to an oligonucleotide containing a 3'phosphate (N14P). C) Representative gel demonstrating dose-dependent inhibition of TDP1 by NSC 88915. D) Graphical representation of the percent inhibition of TDP1 by NSC 88915. Each point represents the mean ± SEM for three independent experiments

- **Furamidine.** *In vitro* biochemical assays also confirmed that furamidine inhibits TDP1 at low micromolar concentrations. Furamidine is known to bind to duplex DNA in the minor groove selectively at AT-rich sites, as well as intercalating between GC base pairs. Since no duplex DNA was present in the screen, the mode of action of furamidine is likely a novel one. Further investigation by surface plasmon resonance (SPR) analysis revealed that furamidine binds not only to DNA duplex, but also to single-stranded DNA, albeit to a lesser degree. Similar analysis also showed that furamidine interacts with TDP1. These results raised the possibility of an inhibitory mode of action by combined interaction to the DNA substrate and to TDP1, which is reminiscent of the interfacial inhibition of Top1cc by Top1 inhibitors.

  Two other diamidine compounds, berenil and pentamidine, are much less effective than furamidine at inhibiting TDP1. Both compounds share the overall curved structure of furamidine, but substitute the furan ring linker in furamidine with other linking groups. This suggests that the furan linker is important in

inhibiting TDP1 activity, potentially by directly interacting with the DNA or TDP1 or both, or by stabilizing the overall curvature of the compound (**Figure 27**) [21].

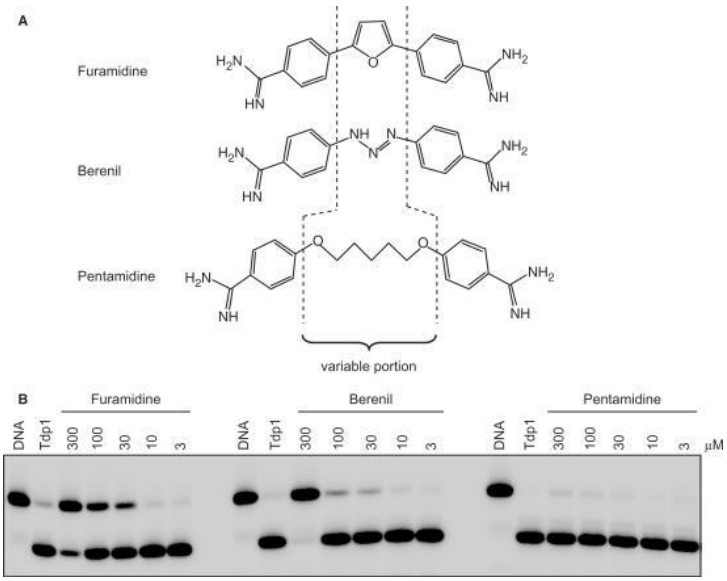

Figure 27. Differential activities of furamidine, berenil and pentamidine against TDP1. (A) Chemical structures of furamidine, berenil and pentamidine. Dashed lines indicate the variable chemical moiety. (B) Reactions were performed with the indicated concentrations (μM) of furamidine, berenil and pentamidine. Reactions were for 20 min at pH 8.0 and 25°C in the presence of 25 nM 14Y substrate and 1 ng of TDP1. Samples were separated on a 20% urea–PAGE gel and visualized.

- **Phosphotyrosine mimetic.** The AlphaScreen (Amplified Luminescence Proximity Homogenous Assay) bead system was used to evaluate the activity of phosphotyrosine mimetic inhibitors. The library of pharmacologically active compounds (LOPAC) was screened to further validate the assay. After data analysis, four active compounds were selected: aurintricarboxylic acid (ATA), the tyrosine phosphatase inhibitor methyl-3,4-dephostatin, and the Gα-specific G-protein antagonists suramin and NF449 (**Figure 28**) [22].

  Suramin blocks the binding of various growth factors, including insulin-like growth factor I (IGF-I), epidermal growth factor (EGF), platelet-derived growth factor (PDGF), and tumor growth factor-beta (TGF-beta), to their receptors, thereby inhibiting endothelial cell proliferation and migration. Both suramin and its analogue NF449 have been recognized as Gsα-selective G protein and P2 receptor antagonists.

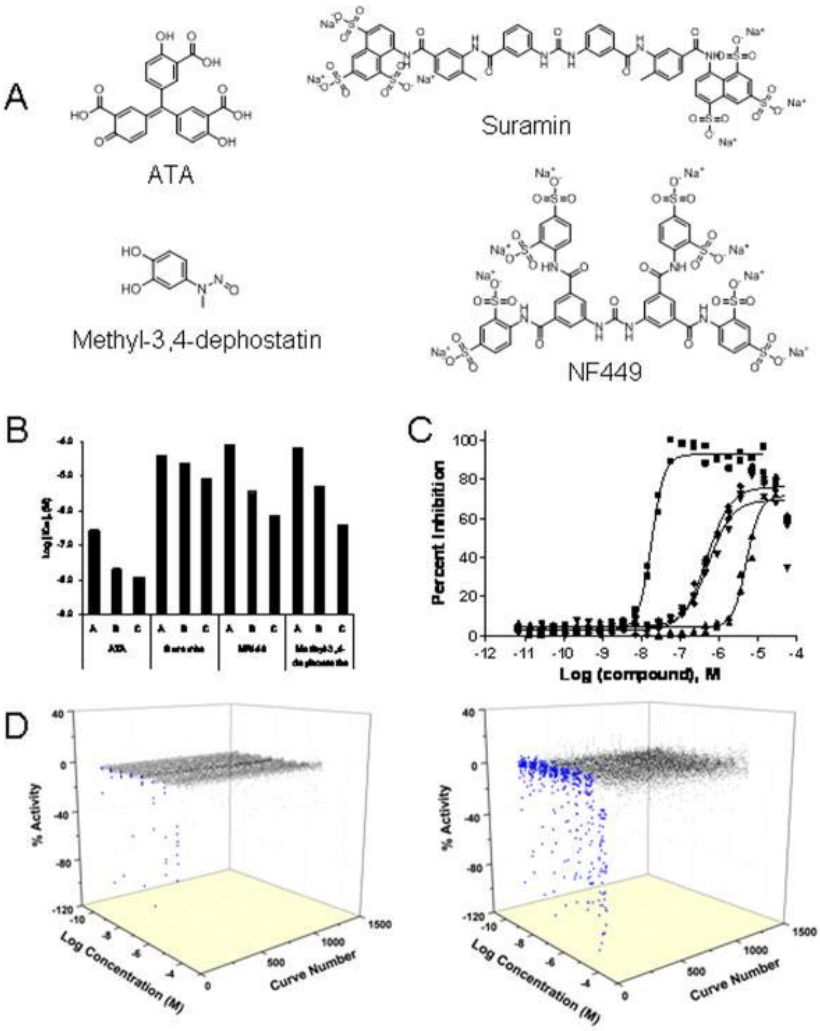

Figure 28. A) Structures of the four hits identified from the pilot screen. B) The hits were tested in dose-response under three reaction conditions: 1 nM enzyme and 5 minute reaction (condition A), 1 nM enzyme and 2 minute reaction (condition B), and 0.2 nM enzyme and 2 minute reaction (condition C). As the substrate conversion decreased, a progressive decrease in IC50 values was observed for all four inhibitors. C) Dose-response curves of the hits tested under condition C. Shown from left to right are the responses for ATA (squares), methyl-3,4-dephostatin (rhombs), NF449 (inverted triangles), and suramin (triangles). D) 3-D scatter plots of qHTS data lacking (black) or showing (blue) concentration–response relationships are shown for the screens of the LOPAC1280 collection performed under conditions of high (left plot, reaction condition A) and low (right plot, reaction condition C) substrate conversion. The increased sensitivity of the second screen is evident from the increase in the number of samples showing stronger inhibition (blue dots).

Herein, they may be acting as decoys, as TDP1 may perceive their extended sulfone group network as multiple phosphotyrosine sites.

The nitrosoaniline, methyl-3,4-dephostatin, is a stable analog of dephostatin and is the smallest of the four active compounds. Of note, it is considerably more potent than vanadate and neomycin. Dephostatin and its analog are known protein tyrosine phosphatase (PTP) inhibitors that also probably act as phosphotyrosine mimetics. Methyl-3,4-dephostatin, in contrast to dephostatin, does not inhibit CD-45 associated PTP, pointing to the exclusivity of the respective binding site. We found that methyl-3,4-

dephostatin inhibited TDP1 at sub-micromolar concentration in both the primary and secondary assays and therefore represents the most potent TDP1 inhibitor reported to date [22].

5.3. TYROSYL-DNA PHOSPHODIESTERASE 2 (TDP2)

Exists another enzyme in human cells that can restore efficiently the 5'-phosphate end to DNA double-strand breaks in preparation for ligation of DNA. This enzyme, TRAF and TNF receptor-associated protein (TTRAP), is a member of the Mg^{2+}/Mn^{2+}-dependent family of phosphodiesterase. Depletion of cellular TTRAP results in increased susceptibility and sensitivity of DNA topoisomerase II-induced double-strand breaks. TTRAP is the first 5'-phosphodiesterase tyrosyl moiety human DNA to be identified, and this enzyme is called tyrosyl-DNA phosphodiesterase 2 (TDP2).

Human TDP2 is smaller than TDP1 with a molecular mass of 41 kDa (362 amino acid residues). Like TDP1, TDP2 is a two-domain protein with the catalytic domain in the C-terminus, while its N-terminal domain bears an ubiquitin-associated (UBA) domain, which probably plays a regulatory role. TDP2 belongs to the exonuclease-endonuclease-phosphatase (EEP) domain nucleases that cleave DNA and RNA backbones. Sequence alignment shows that TDP2 contains four conserved catalytic motifs (TWN, LQE, GDXN and SDH) shared by Mg^{2+}/Mn^{2+}-dependent nucleases, including DNase I and AP endonuclease (APE1). Most residues in all four motifs have been confirmed to be critical for TDP2 (**Figure 29**) [15].

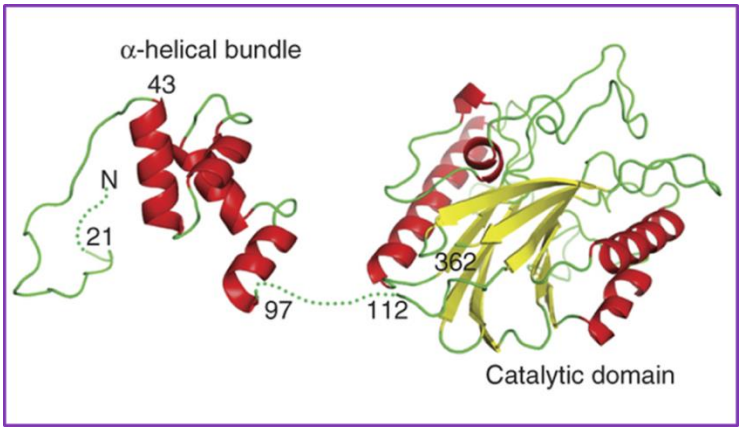

Figure 29. crystal structures of TDP2

Unlike TDP1, TDP2 requires divalent metals, but does not form a transient covalent catalytic intermediate. Mg^{2+}, Mn^{2+}, Co^{2+} are much more efficient than Ca^{2+} or Zn^{2+} for catalysis. The first metal coordinated by residues D262, H351 and N264 also coordinates a deprotonated water molecule for the nucleophilic attack of the phosphate group. The second metal is coordinated by the carboxylic functions of D122 and E152. Residue N120 bridges both metal binding sites by hydrogen bonding with residues E152 and D262. TDP2 generates 5'-phosphate nucleic acid ends, which, unlike the 3'-phosphate TDP1 products, can be readily processed by ligases (**Figure 30**).

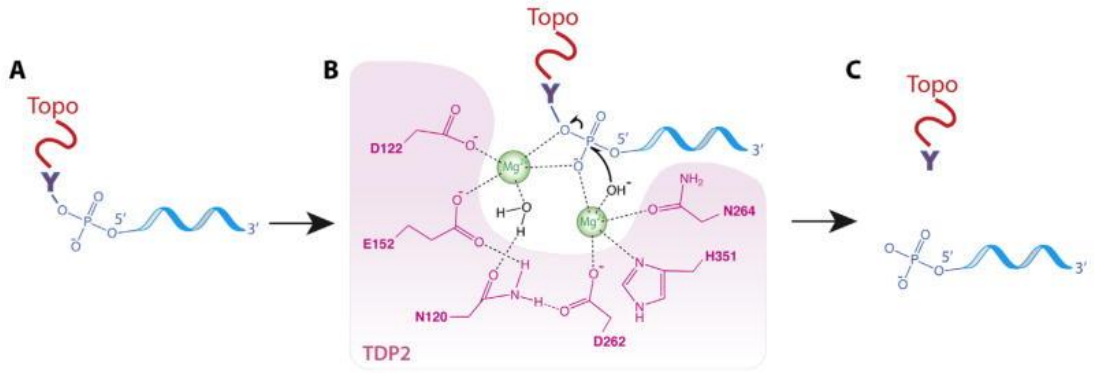

Figure 30. Proposed reaction mechanism for phosphodiester bond cleavage by TDP2. (A) Top2-derived peptide (trapped topoisomerase) linked to 5'-DNA via a phosphotyrosyl bond. (B) Upon binding of the covalent peptide-DNA substrate in the TDP2 active site, two magnesium ions are coordinated by the TDP2 catalytic residues for nucleophilic attack of the phosphotyrosyl bond (black arrows). (C) Cleavage products consisting in the topoisomerase polypeptide (top) and the liberated DNA with a 5'-phosphate end.

TDP2 was recently identified as the host VPg unlinkase for picornaviruses, a large family of viruses including poliovirus, coxackieviruses, rhinoviruses and the classical foot-and-mouth disease virus. TDP2 activity is vital for viral replication, as the 5'-end of the viral genomic RNA of picornavirus is covalently linked to a small (>20 residues) viral protein (VPg) cap via a phosphotyrosyl bond. Upon infection, VPg is removed from the 5'-end of RNA by the 5'-phosphotyrosyl activity of TDP2, thus allowing translation of virus-encoded proteins. Picornavirus family comprises many pathogens responsible for diseases in human and animals, such as polio, common cold, and foot-and-mouth disease. Consequently, inhibitor of TDP2 may serve as treatments for vast populations exposed to these diseases [15].

5.4. TYROSYL-DNA PHOSPHODIESTERASE 2 INHIBITORS

The recently discovered enzyme tyrosyl-DNA phosphodiesterase 2 (TDP2) has been implicated in the topoisomerase-mediated repair of DNA damage. In the clinical setting, it has been hypothesized that TDP2 may mediate drug resistance to Top2 inhibition by etoposide. Therefore, selective pharmacological inhibition of TDP2 is proposed as a novel approach to overcome intrinsic or acquired resistance to Top2-targeted drug therapy. Following a high-throughput screening (HTS) campaign, toxoflavins and deazaflavins were identified as the first reported sub-micromolar and selective inhibitors of this enzyme. Toxoflavin derivatives appeared to exhibit a clear structure-activity relationship (SAR) for TDP2 enzymatic inhibition. However, we observed a key redox liability of this series, and this, alongside early in vitro drug metabolism and pharmacokinetics (DMPK) issues, precluded further exploration. The deazaflavins were developed from a singleton HTS hit. This series showed distinct SAR and did not display redox activity; however, low cell permeability proved to be a challenge [23].

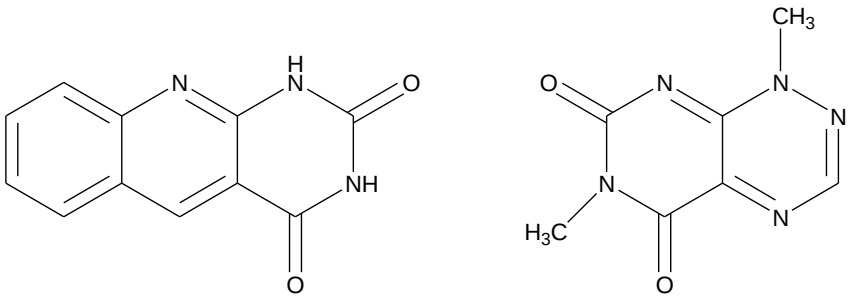

Deazaflavin **Toxoflavin**

Figure 31. TDP 2 inhibitors.

Introduction to experimental section

Cancer, after cardiovascular diseases, is the second cause of death in industrialized countries; it is characterized by an aberrant structure and uncontrolled growth of cells. The current therapy for the treatment of cancer includes surgery, radiotherapy and chemotherapy.

Drugs used as antitumoral agents act by inducing cell cycle arrest or programmed cell death (apoptosis); topoisomerases inhibitors can be listed in the first category.

DNA topoisomerases are essential enzymes inducing DNA modification required during cellular processes such as replication, transcription, repair, etc... Human topoisomerases are classified in type I (Top1) and type II (Top2), depending on whether they cleave single-stranded or double-stranded DNA, respectively. Top1 binds the ribonucleotide chain, leading to the formation of Top1-DNA cleavage complexes (Top1cc). Various conditions can increase the frequency of these complexes, which are converted into DNA damage by cellular metabolism or preexisting DNA lesions. Tyrosyl-DNA phosphodiesterase I (TDP1) is an enzyme that has been implicated in the repair of irreversible Top1-DNA covalent complexes, since it catalyzes the hydrolytic cleavage of the covalent bond between the Top1 catalytic tyrosine and the 3'-end of the DNA.

TDP1 has been regarded as a potential co-target of Top1 for anticancer therapy, in that it seemingly counteracts the effects of Top1 inhibitors, such as camptothecin and its clinically used derivatives. For this reason, TDP1 inhibitors have the potential to enhance the anticancer activity of Top1 inhibitors, by reducing the repair of Top1-DNA lesions.

Within a project aimed to identify new potential TDP1 inhibitors, in collaboration with the group of Professor Pommier of NIH (National Institute of Health, Bethesda), an *in vitro* screening on an *in-house* library of structurally heterogeneous chemical compounds was performed. Three of these molecules (**TDP24**, **RDS2771** and **RDS788**) showed weak inhibitory activity on TDP1, so representing *lead compounds* to be further improved by a lead optimization process.

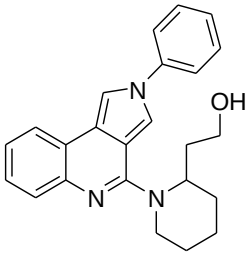

RDS2771

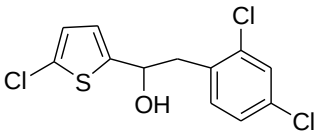

RDS788

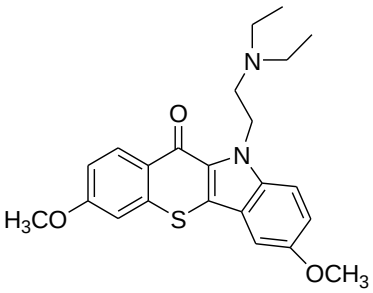

TDP24

These compounds were used as a starting point for a *de novo* design strategy, by means of computational studies conducted in collaboration with the research group of Professor Novellino (University of Naples). Two of the identified hits, **RDS2771** and **TDP24**, are polyaromatic compounds featuring an alkyl chain with a terminal polar group. From these preliminary studies, it is clear that the polar substituents of **TDP24** and **RDS2771** take direct contact with the enzyme residues (**Figure 31**).

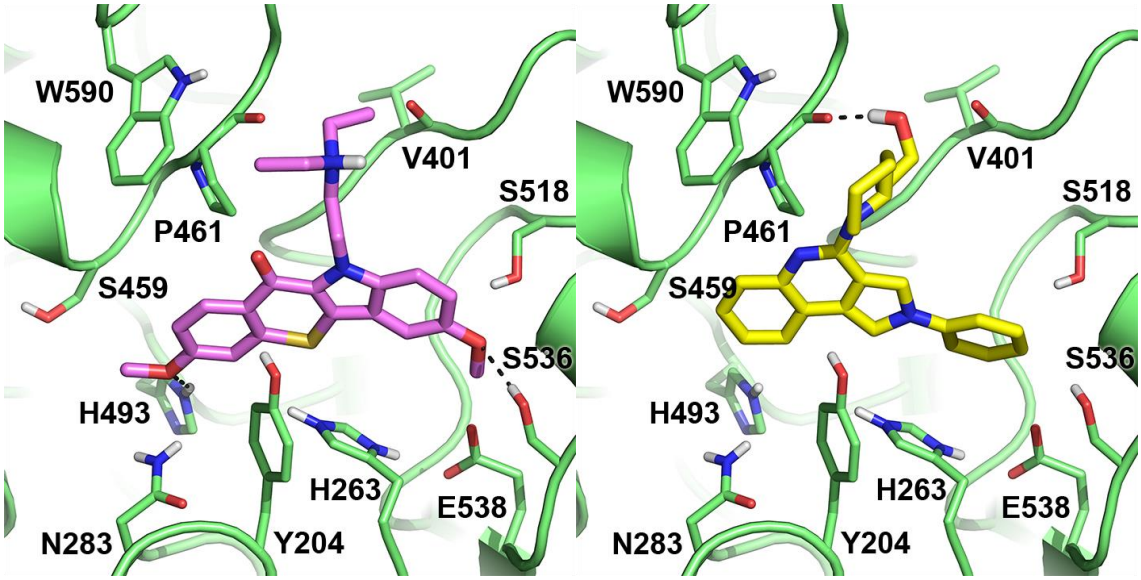

Figure 31. Binding mode of TDP24 (in pink) and RDS2771 (in yellow) predicted in the TDP1 X-ray structure. The protein is represented as green ribbons and sticks.

These ligands contain, within their nucleus, an indole ring (**TDP24**) or a bioisosteric pyrrolopyridine (**RDS2771**), which suggested that properly substituted nitrogen-cointaining heterocyclic derivatives may potentially act as TDP1 inhibitors.

Thus, guided by molecular modeling studies on **TDP24**, a small library of benzothiopyranoindole derivatives **I a-c**, substituted with hydroxylic groups at different positions, has been designed.

The designed ligands were then subjected to molecular docking studies (University of Naples) at the crystal structure of TDP1 (data not shown), that predicted compounds **I a-c** as potential TDP1 binders.

The preparation of the 11-diethylaminoethyl substituted derivatives **I a-c** was performed following the synthetic procedures described in **Schemes 1-3**.

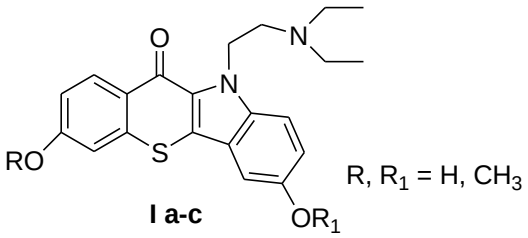

I a-c

The key intermediate 7-methoxy-benzothiopyranone **2** was prepared following previously described procedures (**Scheme 1**) [24].

The first step consisted in the treatment of 3-methoxythiophenol in a 10% NaOH solution with 3-bromopropionic acid in a 10% $NaHCO_3$ solution. The resulting mixture was heated at 60°C for 12 hours to give compound **1**, which was then treated with PPA at 120°C overnight and then poured into ice. The obtained solution was extracted with dichloromethane, yielding compound **2**, that was finally purified by flash chromatography (eluent mixture - AcOEt:petroleum ether 40-60 °C = 2:8).

Scheme 1

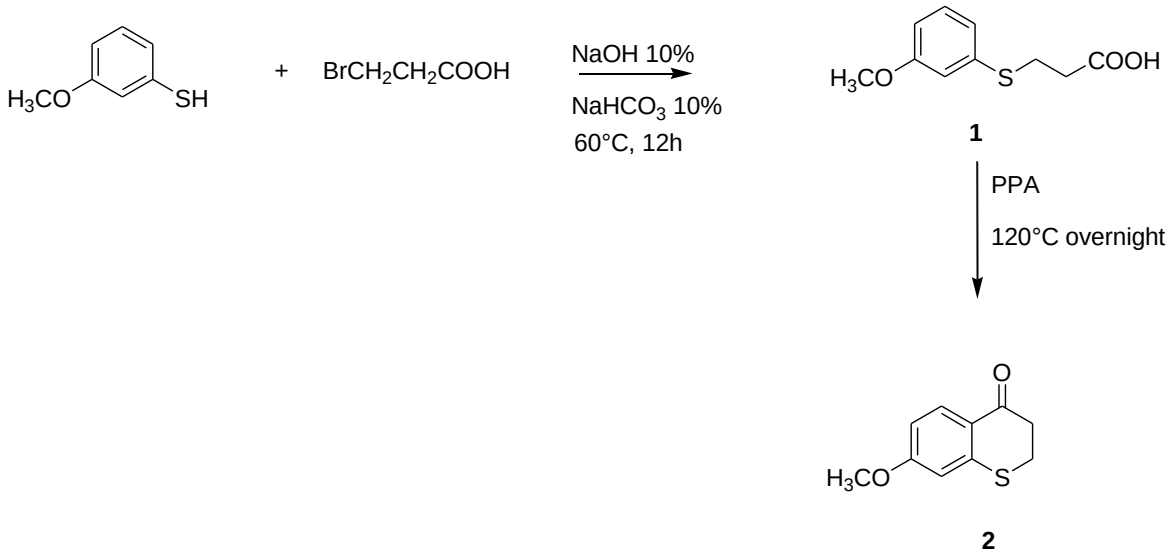

Scheme 2 describes the synthetic procedure followed to obtain compounds **I a-b.**

7-Methoxy-3-hydroxymethylenebenzothiopyranone **3** was obtained by Claisen condensation of compound **2** with ethyl formate in toluene solution, in the presence of sodium methoxide,at room temperature overnight [25-26].

Compound **3**, containing a methine active group, gave the desired 3-phenylhydrazone intermediate **4**, in good yields, by coupling with the *p*-anisidine, previously treated with a 18%solution of HCl and $NaNO_2$ to give the corresponding diazonium salt, using the Japp-Klingemann reaction [27].

Refluxing compound **4** in glacial acetic acid furnished the desired indole **5** in good yields. The solution was poured into ice and the formed solid precipitate was collected by filtration and purified by flash chromatography (eluent mixture - dichloromethane:MeOH = 9:1).

The target 11-*N*-diethylaminoethyl derivative **6** was obtained by reaction of compound **5** with the 2-chloro-*N*,*N*-diethylaminoethyl hydrochloride in anhydrous DMF solution, in the presence of sodium hydride. The mixture was stirred at room temperature overnight. Compound **6** was then purified by flash chromatography (eluent mixture - dichloromethane:MeOH = 9:1).

Finally, compounds **I a-b** were obtained by demethylation of derivative **6** by treatment with boron tribromide, added dropwise in nitrogen atmosphere. At the end, methanol was added to the reaction mixture to hydrolyze the excess of BBr_3, and crude mixture cointaining products **I a-b,** which were separated and purified by flash chromatography (eluent mixture – dichloromethane:MeOH = 9:1).

Scheme 2

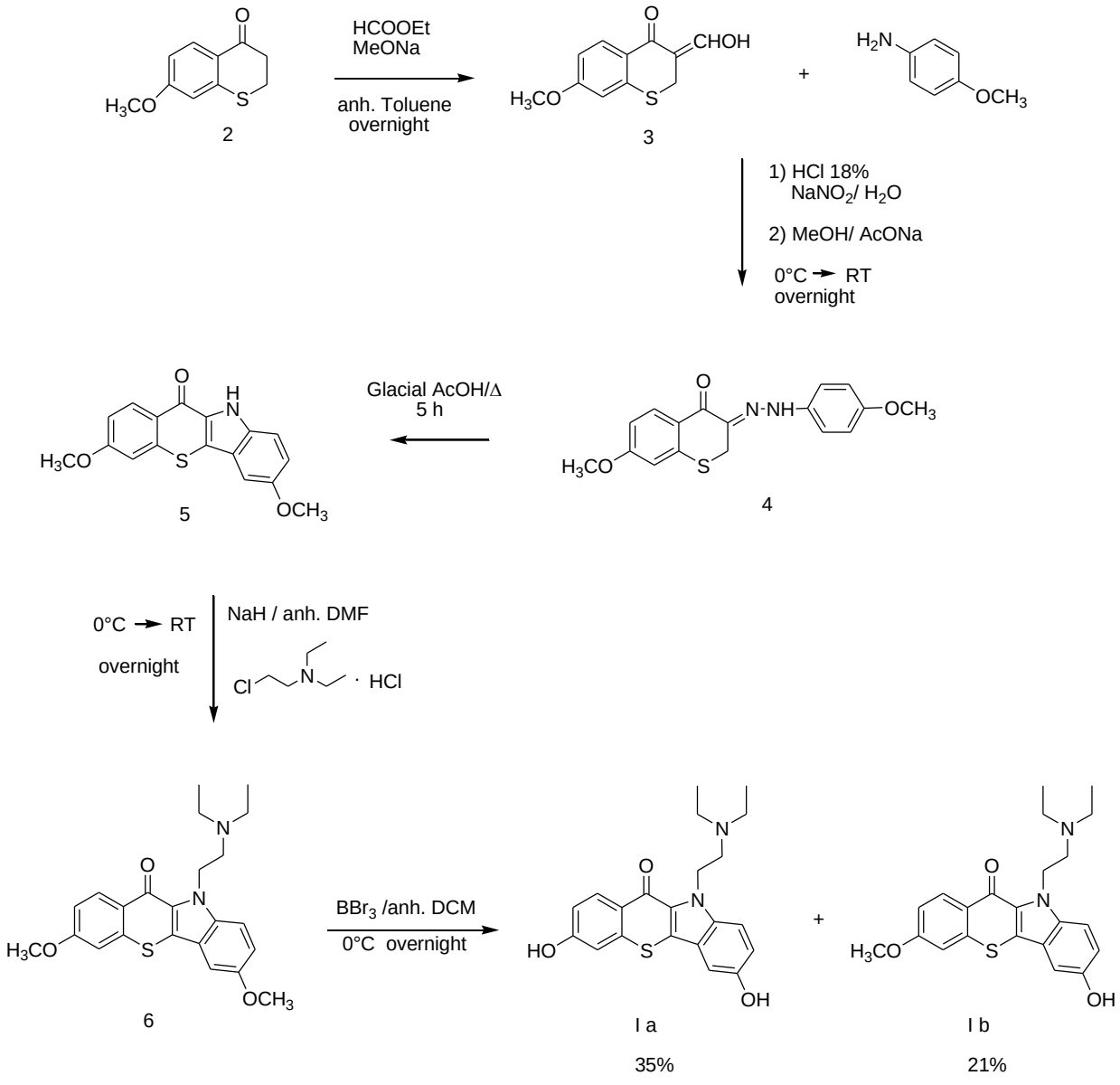

The synthetic procedure for the obtainment of compound **I c** is outlined in **scheme 3**.

7-Hydroxy-benzothiopyranone **7** was obtained by demethylation of derivative **2** with 48% hydrobromic acid. The mixture was heated at 110°C overnight, and then poured into ice. The resulting solid was collected, and purified by flash chromatography (eluent mixture - AcOEt:petroleum ether 40-60 °C = 2:8).

Compound **7** was then treated with benzyl bromide in anhydrous DMF, in the presence of potassium carbonate The yellow mixture was stirred at room temperature for 1 h, poured into a solution of $Et_2O–H_2O$, and stirred for 10 min. The organic layer was separated, dried over Na_2SO_4, filtered, and concentrated to dryness. The crude residue **8** was used in the next reaction without any further purification.

The benzyloxy derivative **8** was formilated by Claisen condensation with ethyl formate in anhydrous toluene solution, in the presence of sodium methoxide, at room temperature overnight to achieve compound **9**. This last derivative contains a methine active group and gave the desired 3-phenylhydrazone intermediate **10**, in good yields, by coupling with the *p*-anisidine, previously treated with a 18% solution of HCl and $NaNO_2$ to give the corresponding diazonium salt, following the Japp-Klingemann reaction [27].

Compound **10** was then directly converted in good yields to the desired indole **11**, by refluxing in glacial acetic acid. The solution was poured into ice and the formed solid precipitate was collected by filtration and purified by recrystallization from toluene to give pure **11**.

The target 11-*N*-diethylaminoethyl derivative **12** was obtained by reaction of compound **11** with 2-chloro-*N*,*N*-diethylaminoethyl hydrochloride in anhydrous DMF solution, in the presence of sodium hydride. The mixture was stirred at room temperature overnight. Compound **12** was purified by flash chromatography (eluent mixture - dichloromethane:MeOH = 9:1) and catalytically hydrogenated over palladium to yield the corresponding phenol derivative **I c**, finally purified by flash chromatography (eluent mixture - dichloromethane:MeOH = 9:1).

Scheme 3

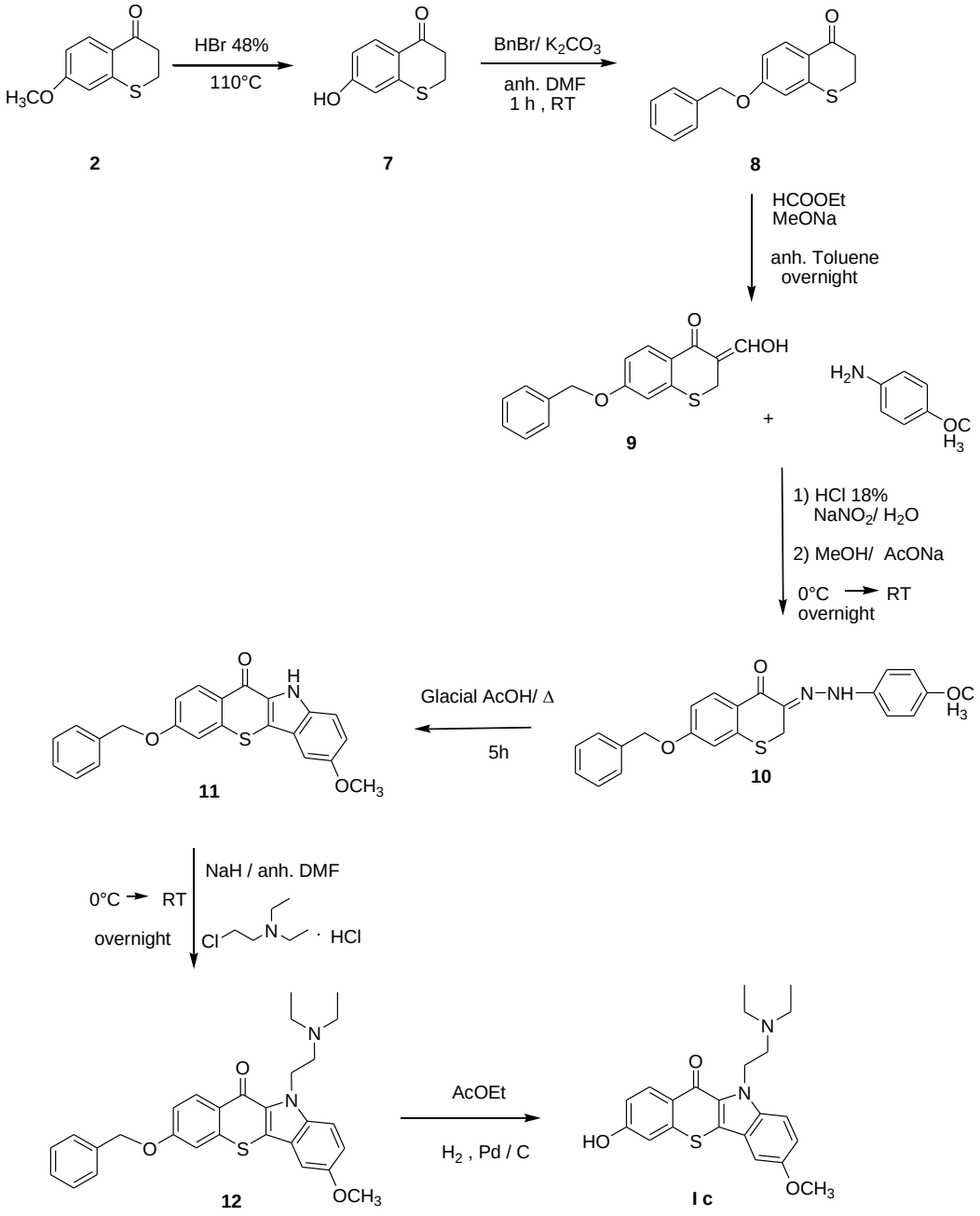
HBr 48%
110°C
BnBr/ K2CO3
anh. DMF
1 h , RT
2
7
8
HCOOEt
MeONa
anh. Toluene
overnight
9
1) HCl 18%
NaNO2/ H2O
2) MeOH/ AcONa
0°C → RT
overnight
10
Glacial AcOH/ Δ
5h
11
NaH / anh. DMF
0°C → RT
overnight
HCl
12
AcOEt
H2 , Pd / C
I c

Experimental section

Melting points were determined using a Reichert Kofler hot-stage apparatus and are uncorrected. Routine nuclear magnetic resonance spectra were recorded in DMSO-d6, MeOD-d6 or CDCl3-d6 solution on a Bruker spectrometer operating at 400 MHz. As drying agent has been used $MgSO_4$. Evaporation was performed in vacuum (rotary evaporator). Analytical TLC was carried out on Merck 0.2 mm percolated silica gel aluminium sheets (60 F-254). Silica gel (230-400 mesh ASTM) was used for column chromatography. Anhydrous reactions were performed in flame-dried glassware under N_2. All reagents used were obtained from commercial sources. All solvents were of an analytical grade.

Procedure for the synthesis of 3-(3-methoxyphenylthio)propanoic acid (1).

2,2 ml (17,82 mmol) of 3-methoxythiophenol were solubilized in a solution of 1,711 g (42,78 mmol) of NaOH in 17,11 ml of distilled water. 3,272 g (21,4 mmol) of 3-bromo-propionic acid were added into a solution of 1,796 g (21,4 mmol) of $NaHCO_3$ in 17,96 ml of distilled water. The two solutions were joined together and the mixture thus obtained was stirred at 60 °C for 12 hours. The resulted solution, after cooling, was extracted with ethyl acetate. The resulting aqueous phase is acidified with HCl to pH 2 and extracted again with dichloromethane. The organic phase was dried with $MgSO_4$, filtered and evaporated at reduce pressure, to achieve 3,261 g (15,36 mmol) of compound **1.**
3-(3-methoxyphenylthio)propanoic acid **1** Yield = 86 %. m.p. = 56-58°C; (lit.ref. n°24; m.p : 58-60°C).

Procedure for the synthesis of 2,3-dihydro-7-methoxythiochromen-4-one (2).

2,00 g (1.0 mmol) of 3-(3-methoxyphenylthio)propanoic acid (**1**) were added with 20.0 g of polyphosphoric acid (PPA). The reaction mixture was heated and stirred at 120 ° C overnight. After cooling, the resulting suspension was poured into ice and the resulted solution was extracted with dichloromethane. The organic phase is dried with MgSO4, filtered and evaporated at reduced pressure. The final product was purified by flash chromatography (AcOEt: Petroleum Ether 40-60 °C = 2:8).
2,3-dihydro-7-methoxythiochromen-4-one **2** Yield = 40%. m.p. = 54-55 ° C (lit.ref. n°24; mp: 55-56 ° C).

Procedure for the synthesis of 2,3-dihydro-3-(hydroxymethylene)-7-methoxythiochromen-4-one (3).

55,5 mg (19.8 mmol) of metallic sodium were solubilized in 5,15 mL of absolute MeOH and the obtained solution, in anhydrous nitrogen current, was added with 7,30 mL of anhydrous toluene. The mixture, cooled in ice, was added dropwise a solution of 2,13 mL (26.4 mmol) of ethyl formiate in 2 mL of anhydrous toluene and, subsequently, 1.282 g (6.60 mmoles) of product **2**, solubilized in 8 mL of anhydrous toluene, was added into the

reaction flask . The resulted solution was stirred at room temperature overnight. After 18 hours (checking by TLC: Toluente / ACCN 9: 1), the mixture obtained is extracted with H2O, and acidified with concentrated HCl. The result was an yellow precipitate which was collected by vacuum filtration to achieve 758 mg (3.41mmoli) of compound **3**.

2,3-dihydro-3-(hydroxymethylene)-7-methoxythiochromen-4-one **3.** Yield: 52%; m.p: 89-92°C(lit.ref. n°25-26; m.p: 90-92 ° C)

.

Procedure for the synthesis of (Z)-3-(2-(4-methoxyphenyl)hydrazono)-2,3-dihydro-7-methoxythiochromen-4-one (4).

To a solution of 605 mg (2,72 mmol) of compound **3** in 15 mL of methanol was added an aqueous saturated solution of 669 mg (8,16 mmol) of sodium acetate. After cooling at 0 °C, a solution of the suitable diazonium salt, obtained from 435 mg (3,53 mmol) of *p*-anisidine in 3,04 mL of 18% hydrochloridric acid and 281 mg (4,07 mmol) sodium nitrite in 3,54 mL of distillated water, was added dropwise. An orange precipitate was immediately formed, and the mixture was stirred for 12 hours at room temperature. The solid was collected and washed with water to give 591 mg (1,80 mmol) crude compounds **4**, whose purity was assessed by TLC analysis (AcOEt: Petroleum Ether 40-60 °C = 2:8).

(Z)-3-(2-(4-methoxyphenyl)hydrazono)-2,3-dihydro-7-methoxythiochromen-4-one **4**. Yield: 66%; m.p: 75-77 °C (lit.ref. n°27; m.p: 74-76°C).

Procedure for the synthesis of 3,7-dimethoxythiochromeno[3,2-b]indol-11(10H)-one (5).

A suspension of compound **4** (486 mg ;1,48 mmol) in 14 mL of glacial acetic acid was heated at 110 °C for 10 hours controlling the progress of the reaction by TLC (dichloromethane : MeOH = 9:1). After cooling , the solution obtained is poured into ice and the obtained suspension was collected by vacuum filtration to give 396 mg (1,27 mmol) compound **5** with good yields**.**

3,7-dimethoxythiochromeno[3,2-b]indol-11(10H)-one **5**. Yield: 85%; m.p: 207-209 °C (ref. m.p: 205-207 °C).

Procedure for the synthesis of 10-(2-(diethylamino)ethyl)-3,7-dimethoxythiochromeno[3,2-b]indol-11(10H)-one (6).

180 mg (0.58 mmol) of compound **5** was added in small portions to a stirred suspension of sodium hydride in 60% dispersion in mineral oil (139 mg, 5,80 mmol) in 10 mL of anhydrous DMF, under nitrogen atmosphere. The reaction mixture was stirred at room temperature for 1 h and then supplemented, at 0 °C, with 150 mg (0,87 mmol) of 2-chloro-*N*,*N*-diethylaminoethyl hydrochloride and left at room temperature for 24 (TLC analysis dichloromethane: MeOH = 9:1). After cooling, the reaction mixture was added dropwise in ice and the crude product precipitated was collected by vacuum filtration and purified by flash chromatography (eluent mixture - dichloromethane:MeOH = 9:1) to achieve 80 mg (0,19 mmol) of compound **6**.

10-(2-(diethylamino)ethyl)-3,7-dimethoxythiochromeno[3,2-b]indol-11(10H)-one **6**. Yield : 51%; m.p: 115-118 °C (lit.ref. n° 27; m.p: 117-118 °C).

Procedure fot the synthesis of 10-(2-(diethylamino)ethyl)-3,7-dihydroxythiochromeno[3,2-b]indol-11(10H)-one (1 a) and 10-(2-(diethylamino)ethyl)-7-hydroxy-3-methoxythiochromeno[3,2-b]indol-11(10H)-one (1 b).

To a solution of compound **6** (0.605 g, 1,47 mmol) in anhydrous dichloromethane (5 ml), cooled at -10°C, was added boron tribromide (2,5 ml, 14,7 mmol) in 1 ml of the same solvent. The mixture was stirred overnight at room temperature (TLC analysis: dichloromethane: MeOH= 9:1). The dichloromethane was evaporated under reduced pressure and the residue was then washed twice with methanol to hydrolyze the excess of BBr3; the crude cointaining products **1 a-b** were finally separated and purified by flash chromatography (eluent mixture- dichloromethane: MeOH= 9:1).

10-(2-(diethylamino)ethyl)-3,7-dihydroxythiochromeno[3,2-b]indol-11(10H)-one **(1 a).** Yield: 35%;

^{1}H-NMR (CD3OD-d6, ppm): 8,50 (d, 1H, J= 9,2 Hz); 7,55 (d, 1H, J= 9,2 Hz); 7,19-7,16 (dd, 1H, J_{min}= 2,4 Hz, J_{max}= 8.8 Hz); 7,13-7,11 (dd, 2H, J_{min}= 2,2 Hz, J_{max}= 7,4 Hz); 7,05-7,02 (dd, 1H, J_{min}= 2,2 Hz, J_{max}= 9,0 Hz); 5,03 (t, 2H, J= 7,0 Hz); 3,39 (t, 2H, J= 6,8 Hz); 3,19 (q, 4H, J= 7,2 Hz); 1,29 (t, 6H, J= 7,2 Hz).

^{13}C-NMR (CD3OD-d6, ppm): 172,99; 160,60; 152,24; 138,54; 134,10; 130,26; 127,15; 124,33; 123,40; 119,29; 118,68; 115,80; 111,17; 110,53; 102,96; 52,32; 40,96; 8,75.

10-(2-(diethylamino)ethyl)-7-hydroxy-3-methoxythiochromeno[3,2-b]indol-11(10H)-one **(1 b)**. Yield : 20%;

^{1}H-NMR (CD3OD-d6, ppm): 8,48 (d, 1H, J= 8,8 Hz); 7,47 (d, 1H, J= 8,8 Hz); 7,22 (d, 1H, J= 2,4 Hz); 7,15-7,10 (m, 3H); 4,92 (t, 2H, J= 8,1 Hz); 3,93 (s, 3H); 3,22 (t, 2H, J= 7,0 Hz); 3,03 (q, 4H, J= 6,3 Hz); 1,23 (t, 6H, J= 7,2 Hz).

^{13}C-NMR (CD3OD-d6, ppm): 172,78; 161,85; 152,15; 138,56; 134,10; 129,85; 127,18; 125,45; 123,30; 119,25; 115,21; 111,20; 108,30; 102,88; 54,98; 52,27; 40,98; 9,18.

Procedure for the synthesis of 7-hydroxythiochroman-4-one (7).

A suspension of compound **2** (905 mg ;4,66 mmol) in 2,74 mL of 48% hydrobromic acid was heated at 120 °C overnight. The resulted mixture, after cooling, was added to ice and the obtained precipitate was collected by vacuum filtration. Compound **7** was then purified by flash chromatography (eluent mixture- AcOEt: Petroleum Ether 40-60 °C = 2:8).

7-hydroxythiochroman-4-one **(7)**. Yield: 25%; m.p: 189-187;

^{1}H-NMR (DMSO-d6, ppm): 7,86 (d, 1H, J= 8,8 Hz); 6,65-6,60 (m, 2H); 3,27-3,24 (m, 2H); 2,81-2,78 (m, 2H).

Procedure for the synthesis of 7-(benzyloxy) -2,3- dihydrothiochromen-4-one (8).

To a solution of compound **7 (**310 mg, 1,7 mmol) in 3 mL of anhydrous DMF**,** was added 0,20 mL of benzyl bromide (1,8 mmol). Subsequently was added potassium carbonate (470 mg, 3,4 mmol). The yellow mixture was stirred at room temperature for 1 h, and then poured into a solution of Et_2O-H_2O, and stirred for 10 min. The ethereal layer was separated. The organic layer was dried over $MgSO_4$, filtered, and concentrated to dryness.

7-(benzyloxy)-2,3-dihydrothiochromen-4-one **(8).** Yield**:** 92%; m.p: 98-100 °C;

^{1}H-NMR (CDCl3-d6, ppm): 8,11 (d, 1H, J= 9,2 Hz); 7,43-7,28 (m, 5H); 6,85 (d,1H, J=2,4 Hz); 6,81-6,79 (dd, 1H, J_{min}= 2,4 Hz, J_{max}= 8.8 Hz); 5,11 (s, 2H); 3,25-3,22 (m, 2H); 2,96-2,93 (m, 2H).

Procedure fot the synthesis of 7-(benzyloxy)-2,3-dihydro-3-(hydroxymethylene)thiochromen-4-one (9).

102 mg (4.44 mmol) of metallic sodium were solubilized in 1,36 mL of absolute MeOH and the obtained solution, in anhydrous nitrogen current, was added with 1,64 mL of anhydrous toluene. The mixture, cooled in ice, was added dropwise a solution of 0,48 mL (5,92 mmol) of ethyl formiate in 2 mL of anhydrous toluene and, subsequently, 400 mg (1,48 mmol) of product **8**, solubilized in 8 mL of anhydrous toluene, was added into the reaction flask . The resulted solution was stirred at room temperature overnight. After 18 hours (checking by TLC: Toluente / ACCN 9: 1), the mixture obtained is extracted with H_2O, and acidified with concentrated HCl. The result was an yellow precipitate which was collected by vacuum filtration to achieve 163 mg (0,55 mmol) of compound **9**.

7-(benzyloxy)-2,3-dihydro-3-(hydroxymethylene)thiochromen-4-one **(9).** Yield: 40%; m.p: 96-98 °C;

^{1}H-NMR (CDCl3-d6, ppm): 8,22 (s, 1H); 7,99 (d, 1H, J= 8,8 Hz); 7,45-7,36 (m, 5H); 6,92 (d, 1H, J= 2,4 Hz); 6,88-6,85 (dd, 1H, J_{min}= 2,4 Hz, J_{max}= 8.8 Hz); 5,13 (s, 2H); 3,69 (s, 2H).

Procedure for synthesis of 3-(2-(4-methoxyphenyl)diazenyl)-7-(benzyloxy)-2,3-dihydrothiochromen-4-one (10).

To a solution of 200 mg (0,67 mmol) of compound **9** in 15 mL of methanol was added an aqueous saturated solution of 165 mg (2,01 mmol) of sodium acetate. After cooling at 0 °C, a solution of the suitable diazonium salt, obtained from 107 mg (0,87 mmol) of *p*-anisidine in 1,11 mL of 18% hydrochloridric acid and 69 mg (1,00 mmol) sodium nitrite in 1,28 mL of distillated water, was added dropwise. An orange precipitate was immediately formed, and the mixture was stirred for 12 hours at room temperature. The solid was collected and washed with water to give 182 mg (0,45 mmol) crude compounds **10**, whose purity was assessed by TLC analysis (AcOEt: Petroleum Ether 40-60 °C = 2:8).

3-(2-(4-methoxyphenyl)diazenyl)-7-(benzyloxy)-2,3-dihydrothiochromen-4-one **(10).** Yield: 67%;

^{1}H-NMR (DMSO-d6, ppm): 7,96 (d, 1H, J= 8,8 Hz); 7,47-7,40 (m, 5H); 7,38-7,33 (m, 2H); 7,10 (d, 1H, J= 2,4 Hz); 7,00-6,98 (dd, 1H, J_{min}= 2,4 Hz, J_{max}= 8.8 Hz); 6,96-6,94 (m, 2H); 5,23 (s, 2H); 4,10 (s, 1H); 3,75 (s, 3H).

Procedure for the synthesis of 3-(benzyloxy)-7-methoxythiochromeno[3,2-b]indol-11(10H)-one (11).

A suspension of compound **10** (89 mg, 0,22 mmol) in 2,1 mL of glacial acetic acid was heated at 110 °C for 10 hours controlling the progress of the reaction by TLC (dichloromethane : MeOH = 9:1). After cooling , the solution obtained is poured into ice and the obtained suspension was collected by vacuum filtration and purified by recrystallization from toluene to give 66 mg (0,16 mmol) of compound **11** with good yields**.**

3-(benzyloxy)-7-methoxythiochromeno[3,2-b]indol-11(10H)-one **(11).** Yields: 74%;

^{1}H-NMR (CD3OD-d6, ppm): 12,28 (s, 1H); 8,52 (d, 1H, J= 9,2 Hz); 7,61 (d, 1H, J= 2,4 Hz); 7,54-7,52 (m, 3H); 7,46-7,42 (m, 2H); 7,39-7,36 (m, 1H); 7,31-7,28 (m, 2H); 7,17-7,15 (dd, 1H, J_{min}= 2,4 Hz, J_{max}= 8,8 Hz); 5,32 (s, 2H); 3,87 (s, 3H).

Procedure for the synthesis of 3-(benzyloxy)-10-(2-(diethylamino)ethyl)-7-methoxythiochromeno[3,2-b]indol-11(10H)-one (12).

81 mg (0,21 mmol) of compound **11** was added in small portions to a stirred suspension of sodium hydride in 60% dispersion in mineral oil (50 mg, 2,1 mmol) in 10 mL of anhydrous DMF, under nitrogen atmosphere. The reaction mixture was stirred at room temperature for 1 h and then supplemented, at 0 °C, with 55 mg (0,32 mmol) of 2-chloro-*N*,*N*-diethylaminoethyl hydrochloride and left at room temperature for 24 (TLC analysis dichloromethane: MeOH = 9:1). After cooling, the reaction mixture was added dropwise in ice and the crude product precipitated was collected by vacuum filtration and purified by flash chromatography (eluent mixture - dichloromethane:MeOH = 9:1).

3-(benzyloxy)-10-(2-(diethylamino)ethyl)-7-methoxythiochromeno[3,2-b]indol-11(10H)-one **(12)**. Yield : 68%;

^{1}H-NMR (MeOD-d6, ppm): 8,33 (d, 1H, J= 8,8 Hz); 7,47-7,33 (m, 6H); 7,10-7,06 (m, 2H); 7,01-6,99 (dd, 1H, J_{min}= 2,6 Hz, J_{max}= 9,0 Hz); 6,95 (d, 1H, J= 2,0 Hz); 5,06 (s, 2H); 4,70 (t, 2H, J= 7,8 Hz); 3,82 (s, 3H); 2,83 (t, 2H, J= 7,6 Hz); 2,73 (q, 4H, J= 7,2 Hz); 1,10 (t, 6H, J= 7,2 Hz).

Procedure for the synthesis of 10-(2-(diethylamino)ethyl)-3-hydroxy-7-methoxythiochromeno[3,2-b]indol-11(10H)-one (I c).

93 mg of derivative **12** (0,19 mmol) was solubilized in ethyl acetate. Subsequently it was added palladium (Pd-C 5%) in slight excess and the mixture was stirred for 24 hours (TLC analysis: dichloromethane: MeOH= 9:1). Compound **1 c** was purified by flash chromatography (eluent mixture - dichloromethane:MeOH = 9:1).

10-(2-(diethylamino)ethyl)-3-hydroxy-7-methoxythiochromeno[3,2-b]indol-11(10H)-one **(I c)**. Yield: 26%;

^{1}H-NMR (MeOD-d6, ppm): 8,50 (d, 1H, J= 9,2 Hz); 7,58 (d, 1H, J= 9,6 Hz); 7,26-7,22 (m, 2H); 7,15 (d, 1H, J= 2,0 Hz); 7,05-7,03 (dd, 1H, J_{min}= 2,4 Hz, J_{max}= 11,2 Hz); 5,00 (t, 2H, J= 7,0 Hz); 3,92 (s, 3H); 3,14 (t, 2H, J= 7,4 Hz); 2,95 (q, 4H, J= 7,1 Hz); 1,18 (t, 6H, J= 7,2 Hz).

References

1. Pontieri, G.M.; *Patologia e Fisiologia Generale*, **2002**, Ed. Piccin, 4-5.
2. Pontieri, G.M.; *Patologia e Fisiologia Generale*, **2002**, Ed. Piccin, 305-370.
3. Bertram G. Katzung, *Farmacologia Generale e Clinica*, Ed. Piccin IV edizione, **2000**, 1005- 1036.
4. Schoeffler AJ, Berger JM; DNA topoisomerases: harnessing and constraining energy to govern chromosome topology, Q Rev Biophys, **2008** Feb, 41(1):41-101.
5. Nitiss J.L., Soans E., Rogojina A., Seth A., Mishina M.; *Topoisomerase assays, Curr Protoc Pharmacol.* **2012** Jun; Chapter 3: Unit 3.3
6. Pommier, Y.; Barcelo, J.M; Rao, V.A.; Sordet, O.; Jobson, A.G.; Thibaut, L.; Miao, Z.H.; Seiler, J.A.; Zhang, H.; Marchand, C.; Agama, K.; Nitiss, J.L.; Redon, C.; Repair of topoisomerase I-mediated DNA damage*, Prog. Nucleic Acid Res. Mol. Biol.*, 81, **2006**, 179-229.
7. James F. Carey, Sharon J. Schultz, Lisa Sisson, Thomas G. Fazzio, and James J. Champoux, DNA relaxation by human topoisomerase I occurs in the closed clamp conformation of the protein*, Proc Natl Acad Sci U S A.,* **2003***; 100: 5640–5645.*
8. Pommier, Y. et. al.; Repair of and checkpoint response to topoisomerase I-mediated DNA damage*, Elsevier,* **2003***, 173-20.*
9. Ivan Laponogov, Dennis A. Veselkov, Isabelle M.-T. Crevel, Xiao-Su Pan, L. Mark Fisher, Mark R. Sanderson*,* Structure of an 'open' clamp type II topoisomerase-DNA complex provides a mechanism for DNA capture and transport, *Nucleic Acids Res*; **2013**; *41* : 9911–9923.
10. Andrew D. Bates, James M. Berger, and Anthony Maxwell; The ancestral role of ATP hydrolysis in type II topoisomerases: prevention of DNA double-strand breaks; *Nucleic Acids Res*.; **2011**; *39* : 6327–6339.
11. Pommier Y.; Topoisomerase I inhibitors: camptothecins and beyond; *Nat Rev Cancer*; **2006**; 6: 789-802.
12. Rozenn Jossé, Scott E. Martin, Rajarshi Guha, Pinar Ormanoglu, Thomas D. Pfister, Philip M. Reaper, Christopher S. Barnes, Julie Jones, Peter Charlton, John R. Pollard, Joel Morris, James H. Doroshow, Yves Pommier; ATR inhibitors VE-821 and VX-970 sensitize cancer cells to topoisomerase I inhibitors by disabling DNA replication initiation and fork elongation responses; *Cancer Res*.; **2014**; *74*: 6968–6979.

13. Yves Pommier; DNA Topoisomerase I Inhibitors: Chemistry, Biology and Interfacial Inhibition; *Chem Rev*.; **2009**; *109*: 2894–2902.
14. Timothy R. Hammonds, Anthony Maxwell, John R. Jenkins; Use of a Rapid Throughput *In Vivo* Screen To Investigate Inhibitors of Eukaryotic Topoisomerase II Enzymes; *Antimicrob Agents Chemother*.; **1998**; *42*: 889–894.
15. Yves Pommier, Shar-yin N. Huang, Rui Gao, Benu Brata Das, Junko Murai, Christophe Marchanda; Tyrosyl-DNA-phosphodiesterases (TDP1 and TDP2); *DNA Repair (Amst).* **2014**; *19*: 114–129.
16. Stefan Gajewski, Evan Q. Comeaux, Nauzanene Jafari, Nagakumar Bharatham, Donald Bashford, Stephen W. White, Robert C.A.M. van Waardenburg; Analysis of the active site mechanism of Tyrosyl-DNA phosphodiesterase I: a member of the phospholipase D superfamily; *J Mol Biol.;* **2012**; *415*: 741–758.
17. Thomas S. Dexheimer, Smitha Antony, Christophe Marchand, Yves Pommier; Tyrosyl-DNA Phosphodiesterase as a Target for Anticancer Therapy; *Anticancer Agents Med Chem*.; **2008**; *8*: 381–389.
18. Trung Xuan Nguyen, Andrew Morrell, Martin Conda-Sheridan, Christophe Marchand, Keli Agama, Alun Bermingam, Andrew G. Stephen, Adel Chergui, Alena Naumova, Robert Fisher, Barry R. O'Keefe, Yves Pommier, Mark Cushman; Synthesis and Biological Evaluation of the First Dual Tyrosyl-DNA Phosphodiesterase I (Tdp1) - Topoisomerase I (Top1) Inhibitors; *J Med Chem*.; **2012**; *55*: 4457–4478.
19. Liao Z, Thibaut L, Jobson A, Pommier Y.; Inhibition of human tyrosyl-DNA phosphodiesterase by aminoglycoside antibiotics and ribosome inhibitors; *Mol Pharmacol.;* **2006**; *70*: 366-72.
20. Thomas S. Dexheimer, Lalji K. Gediya, Andrew G. Stephen, Iwona Weidlich, Smitha Antony, Christophe Marchand, Heidrun Interthal, Marc Nicklaus, Robert J. Fisher, Vincent C. Njar, Yves Pommier; 4-Pregnen-21-ol-3,20-dione-21-(4-bromobenzenesufonate) (NSC 88915) and Related Novel Steroid Derivatives as Tyrosyl-DNA Phosphodiesterase (Tdp1) Inhibitors; *J Med Chem.;* **2009**; *52*: 7122–7131.
21. Shar-yin N. Huang, Pommier Y.; Tyrosyl-DNA Phosdiesterase 1 (Tdp1) Inhibitors; *Expert Opin Ther Pat*.; **2011**; *21*: 1285–1292.

22. Marchand, C.; Lea, W.A.; Jadhav, A.; Dexheimer, T.S.; Austin, C.P.; Inglese, J.; Pommier, Y.; Simeonov, A.; Identification of phosphotyrosine mimetic inhibitors of human tyrosyl-DNA phosphodiesterase I by a novel AlphaScreen high-throughput assay, Mol. Cancer Ther.; **2009;** 240-248.
23. Raoof A, Depledge P, Hamilton NM, Hamilton NS, Hitchin JR, Hopkins GV, Jordan AM, Maguire LA, McGonagle AE, Mould DP, Rushbrooke M, Small HF, Smith KM, Thomson GJ, Turlais F, Waddell ID, Waszkowycz B, Watson AJ, Ogilvie DJ.; Toxoflavins and deazaflavins as the first reported selective small molecule inhibitors of tyrosyl-DNA phosphodiesterase II; *J Med Chem*.; **2013**; *56*: 6352-70.
24. Degani, I.; Fochi, R.; Spunta, G. Heteroaromatic cations. VI. Synthesis Of Thiachromylium Perchlorate Derivatives, *Bollettino Scientifico Della Facoltà Di Chimica Industriale Di Bologna*, **1966** , *24*, 75-91.
25. Marini, *J. Med. Chem*, **2012**, *55*, 9619-9629.
26. Dalla Via L.; *Bioorg. Med. Chem.;* **2009**; *17*: 326-36.
27. Lisa Dalla Via, Sebastiano Marciani Magno, Ornella Gia, Anna Maria Marini, Federico Da Settimo, Silvia Salerno, Concettina La Motta, Francesca Simorini, Sabrina Taliani, Antonio La vecchia, Carmen Di Giovanni, Giuseppe Brancato, Vincenzo Barone, and Ettore Novellino; Benzothiopyranoindole-Based Antiproliferative Agents: Synthesis, Cytotoxicity, Nucleic Acids Interaction, and Topoisomerases Inhibition Properties; *J. Med. Chem*.; **2009;** *52*: 5429–5441.

Ringraziamenti

Ancora non ci credo. Il traguardo che vedevo come irraggiungibile adesso è arrivato.
Gli anni passati all'università mi hanno regalato un sacco di emozioni, positive e negative, che nel complesso mi hanno fatto crescere, maturare dal punto di vista professionale, ma soprattutto come persona . In questi anni ho conosciuto molte persone che hanno reso, nel loro piccolo, migliore il mio percorso universitario, dandomi la forza di andare avanti anche quando vedevo tutto nero o semplicemente regalandomi un sorriso. Vorrei dedicare queste ultime pagine per ringraziare tutte le persone che in me hanno sempre creduto e che mi hanno sempre sostenuto sia nei momenti di difficoltà sia in quelli felici e spensierati.
Vorrei ringraziare in primo luogo la Professoressa Sabrina Taliani che mi ha permesso di intraprendere questo percorso di tesi. Ringrazio inoltre la Dottoressa Elisabetta Barresi, la mia tutor-non-tutor Betti, che mi ha aiutato a portare a termine sintesi a dir poco complesse e che ha contribuito a rendere migliore il mio periodo di tesi con la sua allegria e simpatia. Un grazie arriva anche a Bethesda, al Dottor Marco Robello che non ha potuto seguirmi in tutto questo percorso.
Un ringraziamento speciale va alla mia famiglia che mi è sempre stata accanto non facendomi mai mancare il proprio sostegno e aiutandomi in tutti questi anni. Senza di loro non sarei mai potuta diventare quella che sono adesso. Grazie mamma che sei stata sempre al mio fianco, che mi hai sempre aiutato, dal primo giorno di elementari fino all'ultimo della tesi. Non ti sei mai arresa, anche quando ero "posseduta dal demonio", tu hai creduto in me nelle mie potenzialità e se oggi sono qui è tutto merito tuo. Un grande grazie va anche a te babbo, anche se non potrai esserci fisicamente so che in questo giorno cosi importante ci sarai comunque. Mi hai sempre sostenuta ed hai permesso la realizzazione di questo mio progetto, grazie babbo. Ringrazio anche mio fratello, Andrea che mi è sempre vicino, nel bene e nel male, e anche se spesso non la pensiamo alla stessa maniera, alla fine ci sosteniamo sempre. Ringrazio inoltre il mio ragazzo Simone che mi ha supportato e sopportato, anche quando ero sotto esame ed il nervosismo era

alle stelle, durante tutto questo cammino. Ringrazio inoltre Maya, la mia cucciola, che con il suo amore incondizionato mi ha tirato su il morale in tutti i momenti difficili.

Un sentito grazie va anche ai miei nonni, sempre presenti, che hanno iniziato a chiamarmi dottoressa dal giorno dell'immatricolazione.
Ringrazio inoltre Paola e Fabio che mi hanno adottato, a giorni alterni, durante tutti questi anni e mi hanno sopportato e fatta sentire come a casa mia.
Ringrazio anche tutti i miei amici, conosciuti all'università e non, che mi hanno fatto passare bellissimi momenti durante questo lungo percorso. Ringrazio le mie amiche storiche Ilaria, Jessica e Linda senza le quali non saprei come fare, con la quale ho condiviso momenti bellissimi ed indelebili. Grazie anche alle fanciulle conosciute in tesi, con le quali ho condiviso il laboratorio ed esilaranti avventure. Infine ringrazio la mia collega-compare, Chiara, con la quale ho condiviso ogni momento di questo interminabile percorso, dal test di ingresso alla discussione della tesi. In te ho trovato non solo una collega ma anche una grande amica.